

**STABILITY ANALYSIS BASED ON BIFURCATION  
METHOD: A CASE STUDY OF LAKVIJAYA POWER  
STATION, SRI LANKA**

Jayasuriya Arachchige Thilina Jayaweera

(149283C)

Degree of Master of Science

Department of Electrical Engineering

University of Moratuwa

Sri Lanka

April 2019

**STABILITY ANALYSIS BASED ON BIFURCATION  
METHOD: A CASE STUDY OF LAKVIJAYA POWER  
STATION, SRI LANKA**

Jayasuriya Arachchige Thilina Jayaweera

(149283C)

Thesis/Dissertation submitted in partial fulfilment of the requirements for the degree  
Master of Science in Electrical Engineering

Department of Electrical Engineering

University of Moratuwa

Sri Lanka

April 2019

## Declaration

---

I declare that this is my own work and this thesis does not incorporate, without acknowledgement, any material previously submitted for a Degree or Diploma in any other University or institute of higher learning to the best of my knowledge and belief it does not contain any material previously published or written by another person except where the acknowledgement is made in the text.

Also, I hereby grant to University of Moratuwa the non-exclusive right to reproduce and distribute my thesis, in whole or in part in print, electronic or other medium. I retain the right to use this content in whole or part in future works (such as articles or books).

Signature of the candidate:

.....

J A T Jayaweera

Date:.....

The above candidate has carried out research for the Masters Dissertation under my supervision.

Signature of the supervisor:

.....

Dr. L N W Arachchige

Date:.....

## Abstract

---

The power system is a dynamic system, which consists of nonlinear elements. Generally, methods based on linearization are sufficient to analyse the system under both normal operating conditions and perturbations of the variables. However, due to the stressed operating conditions, system behaviour is highly influenced by the nonlinear elements of the system. Therefore, analysis based on linearized methods is not sufficient to understand the system behaviour under such conditions. In this thesis, a nonlinear analysis is carried out based on bifurcation theories to identify the system behaviour more accurately.

The case study considers the effect of integrating the Lakvijaya power station to the Sri Lankan power system, which can be considered as a small system. Dynamic voltage stability assessment based on bifurcation analysis for both intact and contingency conditions were carried out for a system under consideration. The critical state variables for a bifurcation were identified and mitigation criterions are suggested.

**Keywords:** Bifurcation Analysis, Dynamic Voltage Stability, Hopf Bifurcation, Lakvijaya Power Plant, Saddle Node Bifurcation, Sri Lankan Power System,

## **Acknowledgement**

---

First, I wish to express my sincere gratitude to my supervisor Dr. L N W Arachchige of the Department of Electrical Engineering at University of Moratuwa for her continuous support, encouragement and guidance throughout the research.

I would like to thank Dr. W D Prasad and Dr. H M Wijekoon for their time and effort put in to evaluate my research and especially for their valuable feedback provided during the discussions.

Furthermore, I am thankful to Power Plant Manager, Deputy Plant Managers and Chief Engineers at Lakvijaya Power Plant for their continuous support and encouragement.

I am also grateful to all the lectures of the Department of Electrical Engineering at University of Moratuwa, Sri Lanka for the support extended during the study.

Finally, I would like to express my deepest gratitude to my father, mother and sister for their affection, encouragement and support throughout the period.

# Table of Contents

---

Declaration .....	i
Abstract .....	ii
Acknowledgement .....	iii
List of Figures.....	vi
List of Tables.....	vii
List of Symbols.....	viii
1 INTRODUCTION .....	1
1.1 The Background .....	1
1.2 Problem Statement.....	2
1.3 Objectives.....	2
1.4 Thesis Outline.....	2
2 LITERATURE REVIEW.....	3
2.1 Dynamic System.....	3
2.2 State Space Representation .....	3
2.3 Linearization.....	3
2.4 Power System Stability .....	4
2.5 Voltage Stability .....	5
2.6 Lyapunov Stability Definition.....	6
2.7 Eigenvalues and Stability .....	7
2.8 Bifurcation Theory.....	7
2.9 Saddle Node Bifurcation .....	9
2.10 Hopf Bifurcation.....	9
2.11 Participation Factors .....	11
3 METHODOLOGY .....	14
3.1 Problem Identification .....	14
3.2 Nonlinear Analysis and Method Selection.....	14
3.3 Bifurcation Analysis .....	15
3.4 Developing the Mathematical Model .....	15
3.5 Linearization and Eigenvalue Analysis .....	15
3.6 Numerical Analysis.....	15

4	MODELLING THE SYSTEM.....	16
4.1	Introduction .....	16
4.2	Synchronous Generator Model.....	16
4.3	Exciter Model.....	17
4.4	Load Model .....	17
4.5	Network model .....	18
4.6	System Configuration .....	19
5	RESULTS AND ANALYSIS.....	20
5.1	Test System in Intact Condition .....	20
5.2	Test System in Contingency Condition .....	22
5.3	Bifurcation Analysis .....	24
5.4	Results Validation.....	25
5.5	Participation Factor Analysis .....	31
6	CONCLUSIONS.....	33
6.1	Conclusions .....	33
6.2	Future Directions .....	33
	References .....	34
	Appendix - A: System Modelling.....	37
A.1	Synchronous Generator Model.....	37
A.2	Exciter Model .....	39
A.3	Network Model.....	40
A.4	Power Flow and Load Model .....	42
	Appendix - B: Load Bus Data .....	44
B.1	220 kV Load Bus – Weekend.....	44
B.2	220 kV Load Bus – Weekday.....	45
	Appendix - C: MATLAB Code.....	47
C.1	$Y_{bus}$ Matrix .....	47
C.2	Power Flow Calculation.....	48
C.3	Eigenvalue Movements.....	51

## List of Figures

---

Figure 2.1 : Stability Criteria.....	5
Figure 2.2 : Saddle Node Bifurcation .....	9
Figure 2.3 : Supercritical Hopf Bifurcation .....	10
Figure 2.4 : Subcritical Hopf Bifurcation .....	10
Figure 4.1 : IEEE AC4 Exciter Model.....	17
Figure 4.2 : Network in Intact Condition .....	18
Figure 5.1 : Reactive power Vs Voltage .....	20
Figure 5.3 : Eigenvalue Movement in Intact Network .....	21
Figure 5.2 : Eigen Values .....	21
Figure 5.4 : One Line Outage – New Anuradhapura .....	22
Figure 5.5 : Critical Eigenvalue Movement in Contingency Condition .....	23
Figure 5.6 : Reactive Power Vs Voltage.....	23
Figure 5.7 : Critical Eigenvalues at Subcritical Hopf.....	25
Figure 5.8 : Subcritical Hopf – Stable System .....	26
Figure 5.9 : Rotor Angle Vs Voltage .....	27
Figure 5.10 : Subcritical Hopf – Unstable System .....	27
Figure 5.11 : Subcritical Hopf – Unstable System .....	28
Figure 5.12 : Critical Eigenvalues at Supercritical Hopf.....	29
Figure 5.13 : Supercritical Hopf – Outside the Limit Cycle .....	29
Figure 5.14 : Rotor Angle Vs Voltage – Outside the Limit Cycle .....	30
Figure 5.15 : Rotor Angle Vs Voltage – Inside the Limit Cycle.....	30
Figure 5.16 : Supercritical Hopf – Inside the Limit Cycle.....	31
Figure A.1 : IEEE AC4 Exciter Model.....	39
Figure A.2 : Network in Intact Condition .....	40
Figure A.3 : Network in Contingency Condition .....	42

## List of Tables

---

Table 1.1 : Installed Generation Capacity by Source .....	1
Table 2.1 : Eigen value Stability Criterion.....	7
Table 2.2 : Classification of the Bifurcation .....	8
Table 5.1 : Subcritical Hopf – Largest Participation Factors .....	31
Table 5.2 : Supercritical Hopf – Largest Participation Factors.....	32

## List of Symbols

---

$t$	time
$x, u, y$	state vector, input vector, output vector
$\alpha$	bifurcation parameter
$V$	bus voltage
$\lambda$	eigenvalue
$\sigma, i\omega$	real part and imaginary part of an eigenvalue
$\Delta w_r$	rotor speed derivation from synchronous speed
$w_0$	synchronous speed
$\delta$	generator rotor angle
$\psi_{fd}$	field winding flux
$\psi_{1d}$	direct axis damper winding flux
$\psi_{1q}, \psi_{2q}$	quadrature axis damper winding flux
$P_m$	per unit mechanical power input of a synchronous generator
$P_e$	per unit electrical power output of a synchronous generator
$P_0, Q_0$	static active and reactive component
$P_1, Q_1$	dynamic active and reactive component
$P_2, Q_2$	real and reactive power supplied to the load at bus 2
$P_4, Q_4$	real and reactive power supplied to the load at bus 4
$i_d, i_q$	stator phase currents along d - q axis
$e_d, e_q$	stator voltage along d - q axis
$R_{fd}$	field winding resistance
$R_{1d}$	direct axis damper winding resistance
$R_a$	stator winding resistance
$R_{1q}, R_{2q}$	quadrature axis damper winding resistance
$L_{fd}$	field winding inductance
$L_{1d}$	direct axis damper winding inductance

$L_{1q}, L_{2q}$	quadrature axis damper winding inductance
$L_{adu}$	unsaturated direct axis mutual inductance
$L''_{ads}, L''_{aqs}$	saturated direct axis sub transient mutual inductance
$T'_{d0}, T''_{d0}$	direct axis transient and sub transient open circuit time constant of a synchronous generator
$T'_{q0}, T''_{q0}$	quadrature axis transient and sub transient open circuit time constant of a synchronous generator
$E_{fd}$	field voltage
$E_t$	terminal voltage
$T_a, T_b, T_e$	exciter time constants for regulator and lead lag compensator
$k_1$	exciter gain
$Y_{ij}$	$i j^{\text{th}}$ element of $Y_{\text{bus}}$ matrix
$V_2, \delta_2$	voltage magnitude and the angle at bus 2
$V_4, \delta_4$	voltage magnitude and the angle at bus 4

# 1 INTRODUCTION

This chapter presents an introduction of Sri Lankan power system and the role of the Lakvijaya power station. In addition, problem statement and objectives of this study are presented here.

## 1.1 The Background

Increasing electrical power demand urges effective utilization of all the available resources such as power plants, transmission lines and substations to maximize the performance and reduce the cost. In order to deliver power while fulfilling the above criteria, operation conditions of power plants and other equipment need to be planned well and conform to operate within their limits. Sri Lankan power system comprised of 4087 MW installed capacity with the diversified generation mix as in Table 1.1 [1].

Table 1.1 : Installed Generation Capacity by Source

Source	Installed Capacity (MW)
Major Hydro	1391
Mini Hydro	354
Thermal – Oil	1233
Thermal – Coal	900
Other Renewable	209
Total	4087

Source: “Statistical Digest,” Ceylon Electricity Board, 2017

AC transmission network consists of 220 kV (total length of 601 km) and 132 kV (total length of 2313 km including both overhead and underground) lines. Distribution network at 33 kV and 11 kV covers around 33269 km and around 99.7% of the country is electrified [2].

In order to diversify the fuel mix in the generation as planned, on March 2011, phase one of the Lakvijaya coal fired power plant was commissioned. Phase two was added to the system on May 2014, providing 900 MW total. Power station consists of three, two pole, cylindrical rotor, synchronous generators with a capacity of 353 MVA each connected to a steam turbine. Generated voltage at 20 kV is converted to 220 kV using 360 MVA step up transformers and connected to the national grid through two double circuit transmission lines. Currently, on a typical day (24 hrs), Lakvijaya power plant provides more than 50% of the total energy requirement of Sri Lanka.

## 1.2 Problem Statement

To get the optimal utilisation of available capacities, it is required to operate the system near its stability margins. Therefore, it is vital to have a good understanding on stability boundaries and behaviour of system stability based on operational conditions. Power system is a nonlinear system comprised of a large number of variables and hence analyzing its stability using linearized methods will not give precise details when the nonlinearities become prominent. Therefore, it is essential to use non-linear analysis methods to get proper understanding of the system and its transient performance.

## 1.3 Objectives

The main objective of this research is to evaluate the parameters affecting the power system stability when integrating a large power plant to a small power system. Mainly, how to determine the voltage stability region accurately in a given bus and its relationship to machine parameters is evaluated. Specific objectives are,

- To develop a mathematical model to evaluate power system voltage stability
- To determine the stability region accurately considering the nonlinearities in the power system
- To apply the proposed method to evaluate the parameters affecting power system stability in integrating Lakvijaya power station to the Sri Lankan power system

## 1.4 Thesis Outline

The thesis is divided into six chapters as follows;

Chapter 2 – This gives a complete review on literature related to analysing the nonlinear system using nonlinear techniques. Stability criterion of the system based on Lyapunov definitions and eigenvalues based techniques are also presented.

Chapter 3 – Presents the methodology used to achieve the identified objectives of the study. Each step described briefly.

Chapter 4 – Gives a complete overview of modelling the system. Technical aspects of each element are discussed here.

Chapter 5 – Present the results of the study based on analysis considering both intact and contingency situation of a system. Analysis based on both traditional eigenvalue method and nonlinear bifurcation method is presented.

Chapter 6 – Recapitulate major findings of the study and present future directions

## 2 LITERATURE REVIEW

---

This chapter presents a comprehensive review of literature related to the subject area of the nonlinear dynamics and bifurcation theory.

### 2.1 Dynamic System

Dynamic system is a system in which the state continuously changes with time. These changes are governed by a set of rules that specify the states of the system for either discrete (governed by algebraic equations) or continuous (governed by differential equations) values of time.

### 2.2 State Space Representation

Formulating a system model is vital to get proper representation of the system behaviour under the transient and sub transient conditions. State space can be identified as a normalized space of independent coordinates required to describe the behaviour of the dynamic system. These independent coordinates are called the state variables and it is the smallest set of variables that required to represent the system. A nonlinear system can be described by a set of differential and algebraic equations as in Equation (2.1) and (2.2) respectively [3] [4].

$$\dot{x} = F(x, u, t) \quad 2.1$$

$$y = G(x, u, t) \quad 2.2$$

Here  $x$  represents the states and  $u$  represents the inputs of the system. Inputs and states can be any number that required to represents the system accurately. Using vector matrix notation for a system having  $n$  states and  $m$  inputs,  $x$ ,  $u$  and  $F$  can be represented by

$$x = \begin{bmatrix} x_1 \\ x_2 \\ \vdots \\ x_i \\ \vdots \\ x_n \end{bmatrix}, \quad u = \begin{bmatrix} u_1 \\ u_2 \\ \vdots \\ u_i \\ \vdots \\ u_m \end{bmatrix}, \quad F = \begin{bmatrix} F_1 \\ F_2 \\ \vdots \\ F_i \\ \vdots \\ F_n \end{bmatrix} \quad 2.3$$

In both Equations (2.1) and (2.2), time is denoted by  $t$ . If the derivatives of the state variables (i.e.  $\dot{x}$ ) are not explicitly depend on time, the system is said to be autonomous or otherwise non-autonomous [5].

### 2.3 Linearization

It is possible to linearize the nonlinear system equation about the equilibrium point as follows [5]. In Equation (2.1), if  $x_0$  and  $u_0$  are the state and input vectors respectively, which satisfy the equilibrium of the system, then,

$$\dot{x} = F(x_0, u_0) = 0 \quad 2.4$$

With small deviation to the above equilibrium point,

$$x = x_0 + \Delta x, \quad u = u_0 + \Delta u \quad 2.5$$

Substituting the Equation (2.1),

$$\dot{x} = \dot{x}_0 + \Delta \dot{x} = F[(x_0 + \Delta x), (u_0 + \Delta u)] \quad 2.6$$

Using Taylor's series expansion and neglecting higher derivatives following equations can be obtained;

$$\Delta \dot{x}_i = \frac{\partial F_i}{\partial x_1} \Delta x_1 + \dots + \frac{\partial F_i}{\partial x_n} \Delta x_n + \frac{\partial F_i}{\partial u_1} \Delta u_1 + \dots + \frac{\partial F_i}{\partial u_m} \Delta u_m \quad 2.7$$

$$\Delta y_j = \frac{\partial G_j}{\partial x_1} \Delta x_1 + \dots + \frac{\partial G_j}{\partial x_n} \Delta x_n + \frac{\partial G_j}{\partial u_1} \Delta u_1 + \dots + \frac{\partial G_j}{\partial u_m} \Delta u_m \quad 2.8$$

Where  $i = 1, 2, \dots, n$  and  $j = 1, 2, \dots, m$

This can be written as,

$$\Delta \dot{x} = A \Delta x + B \Delta u \quad 2.9$$

$$\Delta y = C \Delta x + D \Delta u \quad 2.10$$

Where,

A is the state matrix of size  $n \times n$

B is the input matrix of size  $n \times m$

C is the output matrix of size  $m \times n$

D is the feed forward matrix of size  $m \times m$

## 2.4 Power System Stability

Stability of a system can be broadly characterised as steadiness, firmness or strength to stand without being overthrown. An equilibrium point of the dynamic system is a point in a state plane where there is a constant state of the system at all the time. This equilibrium point can be stable or unstable depending on the behaviour of the state variables and the inputs. Three quantities are important in power system operation

i.e. Power angle, Frequency and the Voltage. Based on these quantities, power system stability can be divided into three subsets (Figure 2.1). Rotor angle stability is to maintain synchronism through torque balance (between electromagnetic torque and mechanical torque) of generators connected to the system. Frequency stability is the ability to maintain steady frequency when the power system undergoes significant imbalance between generation and load. Voltage stability is the ability to maintain steady acceptable voltage following a system disturbance. Voltage instability can cause through reactive power unbalance and rotor angle instability. It is also important to note that due to the nonlinear nature of the power system, stability depends on both the initial condition of the system and the nature of the disturbance [3] [6].

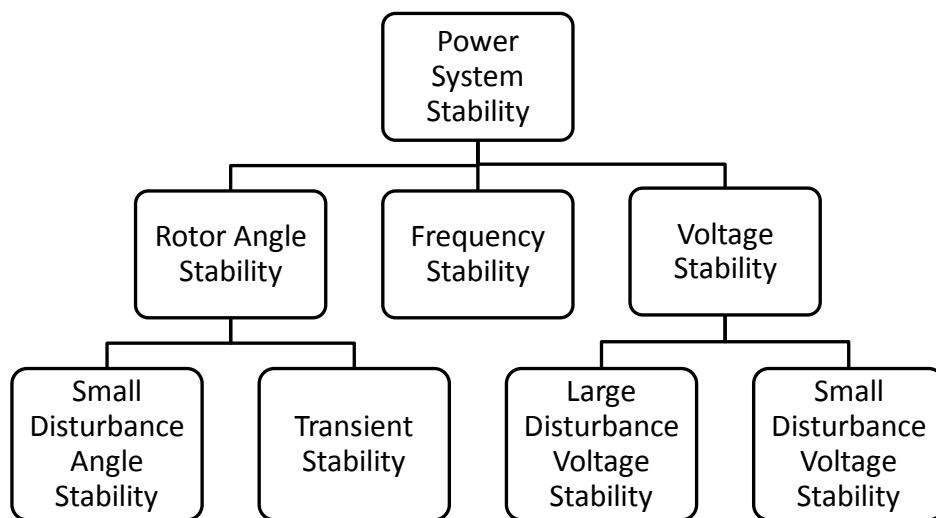


Figure 2.1 : Stability Criteria

## 2.5 Voltage Stability

Voltage stability refers to the ability of the power system to maintain steady voltages at all buses in the system after being subjected to a disturbance from a given initial operating condition [7]. Voltage instability is generally caused by a stressed system resulting progressive fall or rise of voltage of some buses in the power network. The main factor for this instability is the inability of the system to meet the demand for reactive power. Voltage stability can be classified under the following subcategories.

Large disturbance voltage stability is defined as the ability to maintain voltage stability after the large disturbance such system faults, loss of generation or circuit contingencies. Small disturbance voltage stability is defined as the ability to maintain stability after small perturbations. These criterions can be further divided into two

based on time as short term and long term stability [5] [7]. Many voltage instability phenomena have been reported in recent past where some were leading to the cascade failures of the system [8] [9] [10]. Increase in the demand for the electric power forces the transmission network to operate near its margins. Further, the excessive usage of equipment such as low inertia compressor motors and power electronic controllers in both household and industries have a negative impact on voltage stability of the system.

## 2.6 Lyapunov Stability Definition

There are several theories that define and characterize the stability of a system. However, the Lyapunov stability definitions and related theories are most commonly used in defining a stability of a nonlinear system especially in power system.

Consider the Equation (2.1) where  $x$  is a state vector. All the control inputs are assumed to be known functions of the system states and time. Assume equilibrium point of Equation (2.1) to be,  $x = 0$ :

- Stable if for each  $\epsilon > 0$ , there is  $\delta = \delta(\epsilon, t_0) > 0$  such that;

$$\|x(t_0)\| < \delta \Rightarrow \|x(t)\| < \epsilon, \forall t \geq t_0 \geq 0$$

- Uniformly stable if, for each  $\epsilon > 0$ , there is  $\delta = \delta(\epsilon) > 0$ , independent of  $t_0$ , such that;

$$\|x(t_0)\| < \delta \Rightarrow \|x(t)\| < \epsilon, \forall t \geq t_0 \geq 0$$

- Unstable if not stable
- Asymptotically stable if it is stable and in addition there is  $\eta(t_0) > 0$  such that;

$$\|x(t_0)\| < \eta(t_0) \Rightarrow x(t) \rightarrow 0 \text{ as } t \rightarrow \infty$$

- Uniformly asymptotically stable if it is uniformly stable and there is  $\delta_0 > 0$ , independent of  $t_0$ , such that for all

$$\|x(t_0)\| < \delta_0, x(t) \rightarrow 0 \text{ as } t \rightarrow \infty$$

Uniformly in  $t_0$  and  $x(t_0)$ , that is for each  $\epsilon > 0$ , there is  $T = T(\epsilon, \delta_0) > 0$  such that;

$$\|x(t_0)\| < \delta_0 \Rightarrow \|x(t)\| < \epsilon, \quad \forall t \geq t_0 + T(\epsilon, \delta_0)$$

If a system is asymptotic stable, regardless of starting point, system will eventually return to the equilibrium point after a disturbance. On the other hand, in uniformly asymptotical stable system, it will not return to the equilibrium point but demonstrate stable oscillations.

## 2.7 Eigenvalues and Stability

It is possible to define a scalar parameter (say  $\lambda$ ) such a way that there exist non trivial solutions for the Equation (2.11).

$$A\phi = \phi\lambda \quad 2.11$$

$$\det(A - \lambda I) = 0 \quad 2.12$$

Where,

$A$  – System matrix of  $n \times n$

$\phi$  – Vector of  $n \times 1$

$I$  – Identity Matrix

By solving the Equation (2.12), it is possible to find  $n$  number of solutions for the scalar  $\lambda$ , which is identified as eigenvalue of system matrix  $A$ . It should be noted that the number of eigenvalues are equal to the number of state variables in the system matrix. In general, eigenvalues can be written in a form of  $(\sigma + i\omega)$  and depending on the value of  $\sigma$  and  $\omega$  the stability of a system matrix can be defined as in Table 2.1 [5].

Table 2.1 : Eigen value Stability Criterion

Eigen value Type	Stability	Oscillatory Behaviour	Notation
All real and positive	Unstable	None	Nodal Source
All real and negative	Stable	None	Nodal sink
Mixed real	Unstable	None	Saddle point
$\sigma + i\omega$	Unstable	Un-damped	Spiral source
$-\sigma + i\omega$	Stable	Damped	Spiral sink

## 2.8 Bifurcation Theory

Although the bifurcation theory has a classical mathematical background from the works of a Swiss mathematician Leonhard Euler (1744), its modern development begins with a French mathematician Jules H. Poincare (1900). The meaning of the bifurcation is some sort of branching process. This is used extensively to describe any process in which the quantitative or topological behaviour of the object, which is under consideration, alters with the change of a parameter on which the object

depends. In order to get a clear idea about the bifurcation and related sub theories following terms need to be defined.

Orbits – These are the curves in the state space parameterised by the time and oriented by its direction of increase governed by the system equations under consideration. Basically, this is another representation of a system either the continuous or discrete [11].

Phase portrait – This is a diagram, which partition the state space of a dynamic system into orbits. By doing so, it is possible to identify the dynamic behaviour of the system under consideration qualitatively [11].

Limit cycle – This is a periodic solution or a periodic orbit of a dynamic system. The system is in a dynamic steady state when the trajectory of the system approaches a closed curve and remains there for  $t \geq t_0$ . This closed cycle, towards which the trajectory wind, is identified as the limit cycle [11].

Equation (2.13) shows the continuous dynamic equation where  $x$  is a variable and  $\alpha$  is a parameter. When the parameter changes, the phase portrait of the system also changes. This change might be either topologically equivalent or not equal to the original phase portrait. The appearance of a topologically non equivalent phase portrait under variation of parameters is called the Bifurcation [12].

$$\dot{x} = F(x, \alpha) \tag{2.13}$$

Therefore, the bifurcation is a change of the phase portrait of the system as the parameter under consideration is changed. The particular value of the parameter that changes the topology is defined as bifurcation value (or critical value). Bifurcation can be broadly divided as a global and local bifurcation. Under these clarifications, there are several types of bifurcation phenomena exist (Table 2.2) [13] [14]. In this research, only the saddle node bifurcation and Hopf bifurcation were considered.

Table 2.2 : Classification of the Bifurcation

Global Bifurcation	Local Bifurcation
<ul style="list-style-type: none"> <li>• Homoclinic</li> <li>• Heteroclinic</li> <li>• Infinite period</li> </ul>	<ul style="list-style-type: none"> <li>• Saddle node</li> <li>• Transcritical</li> <li>• Pitchfork</li> <li>• Period doubling</li> <li>• Hopf</li> </ul>

## 2.9 Saddle Node Bifurcation

Consider Equation (2.13); As discussed in the Section 2.8,  $\alpha$  is the system parameter and assume that at  $\alpha = 0$ , the system is in equilibrium with  $\mathbf{x}_0 = 0$ ,  $\lambda_1 = 0$  and  $\lambda_2 < 0$ , where  $\lambda_1, \lambda_2$  are eigenvalues. It can be proven that, under the given conditions, Equation (2.13) can be decoupled into two locally topologically equivalent equations. Further, it can be proven that the phase portraits of the decoupled system depend on a selected parameter. The system has two hyperbolic equilibria when  $\alpha < 0$ . One is a stable node, (Figure 2.2 (a)) and other is a saddle point (Figure 2.2 (b)). At  $\alpha = 0$  these two points collide each other and form the saddle node point. If the parameter increased further i.e.  $\alpha > 0$  system will not have any equilibrium point [15].

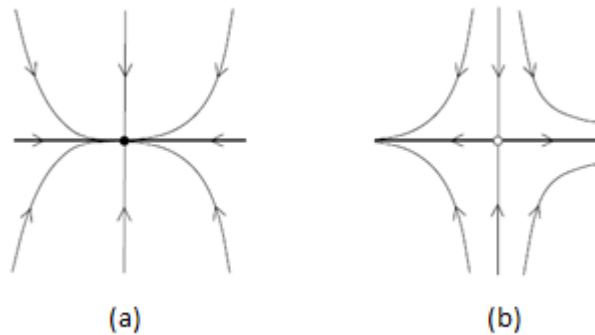


Figure 2.2 : Saddle Node Bifurcation [12]

## 2.10 Hopf Bifurcation

Assume that the system is at hyperbolic equilibrium where  $\mathbf{x} = \mathbf{x}_0$  when the parameter  $\alpha = \alpha_0$  in Equation (2.13). It can be seen that under the small variation of the parameter  $\alpha$ , equilibrium changes slightly but the topology remains hyperbolic. If the parameter changes further, there are two possible situations where hyperbolic topology can be violated: simple real eigenvalues approaches zero or pair of complex eigenvalues reaches the imaginary axis.

There are two eigenvalues such that  $(\lambda_{1,2} = \pm j\omega)$ , where  $\omega > 0$ , when the latter condition is fulfilled. The bifurcation associated with this condition is defined as Hopf bifurcation. This can be described as if the system is having a complex pair of eigenvalues, which crosses imaginary axis with non-zero speed with the change of the parameter, a unique periodic solution appears or disappears. Hopf bifurcation can be divided into two subclasses. i.e. Supercritical Hopf and Subcritical Hopf bifurcation.

Supercritical Hopf Bifurcation - A Hopf bifurcation that forms a stable limit cycle. When supercritical bifurcation occurs, stable limit cycle exists around the unstable equilibrium point (Figure 2.3)

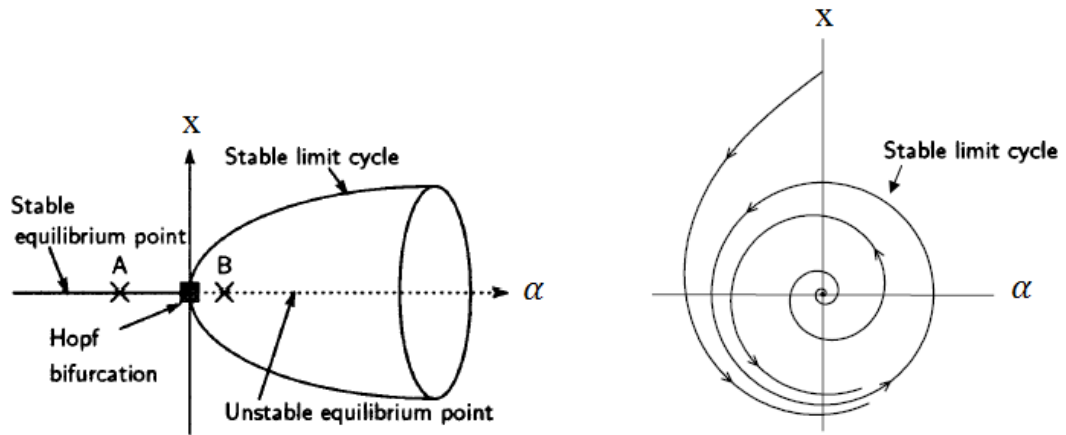


Figure 2.3 : Supercritical Hopf Bifurcation [12] [16]

Consider the point **A** in Figure 2.3. At this point, the system is stable. With the change in the parameter  $\alpha$  system moves to the operating point **B**. As long as the system is not undergoing any disturbance, it will stay at point **B**. But, the point **B** is not stable, and if the system experiences any small disturbance, it will lose its original position and exhibit sustained oscillations (Uniformly asymptotically stable) [17] [16].

Subcritical Hopf Bifurcation – In this bifurcation, an unstable limit cycle exists around the stable equilibrium point.

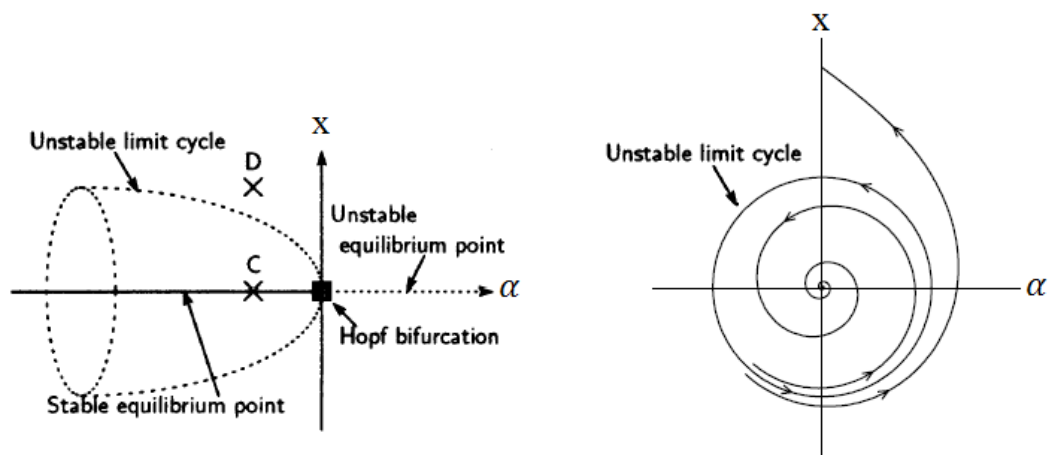


Figure 2.4 : Subcritical Hopf Bifurcation [12] [16]

Consider the system is operating at point **C** in the Figure 2.4. Then the system is stable and it can sustain small disturbances without losing stability. On the other hand, a small disturbance can make the system unstable if the system is at point **D** (i.e. outside the limit cycle). Therefore, the stability region is defined by the limit cycle and any operating point outside is not stable. When the disturbance happened, the system will move further from the equilibrium point and exhibit un-sustained oscillations. [17] [16].

### 2.11 Participation Factors

As discussed in Section 2.7, a scalar parameter ( $\lambda$ ) and a non zero column vector ( $\phi$ ) can be defined such a way that it will satisfy Equation (2.11). Vector  $\phi$  is a right eigenvector (Equation 2.14) [5] associated with the eigenvalue  $\lambda$ .

$$\phi_i = \begin{bmatrix} \varphi_{1i} \\ \varphi_{2i} \\ \cdot \\ \varphi_{ii} \\ \cdot \\ \varphi_{ni} \end{bmatrix} \quad 2.14$$

For an every eigenvalue and a related eigenvector, Equation (2.11) holds and if there are  $n$  numbers of eigenvalues corresponding to the  $n$  numbers of state variables,

$$A [\phi_1 \phi_2 \dots \phi_i \dots \phi_n] = [\phi_1 \phi_2 \dots \phi_i \dots \phi_n] \begin{bmatrix} \lambda_1 & 0 & \cdot & 0 & 0 \\ 0 & \lambda_2 & \cdot & 0 & 0 \\ \cdot & \cdot & \cdot & \cdot & 0 \\ \cdot & \cdot & \cdot & \lambda_i & \cdot \\ 0 & 0 & \cdot & 0 & \lambda_n \end{bmatrix} \quad 2.15$$

$$A\Phi = \Phi\Lambda \quad 2.16$$

Where,

$$\Phi = [\phi_1 \phi_2 \dots \phi_i \dots \phi_n]$$

$$\Lambda = \begin{bmatrix} \lambda_1 & 0 & \cdot & 0 & 0 \\ 0 & \lambda_2 & \cdot & 0 & 0 \\ \cdot & \cdot & \cdot & \cdot & 0 \\ \cdot & \cdot & \cdot & \lambda_i & \cdot \\ 0 & 0 & \cdot & 0 & \lambda_n \end{bmatrix}$$

$\Phi$  is a square matrix and  $\Lambda$  is a diagonal matrix of the eigenvectors and eigenvalues of the state matrix  $A$  respectively. It can be proven that for the distinct eigenvalues of the particular state matrix, corresponding eigenvectors are linearly independent. Therefore  $\Phi$  is a non singular matrix and the inverse ( $\Psi$ ) exists (Equation 2.17).

$$\Phi^{-1} = [\phi_1 \ \phi_2 \ \dots \ \phi_i \ \dots \ \phi_n]^{-1} = \Psi = \begin{bmatrix} \psi_1 \\ \psi_2 \\ \vdots \\ \psi_i \\ \vdots \\ \psi_n \end{bmatrix} \quad 2.17$$

$$\psi A = \psi \lambda \quad 2.18$$

Further,

$$\begin{bmatrix} \psi_1 \\ \psi_2 \\ \vdots \\ \psi_i \\ \vdots \\ \psi_n \end{bmatrix} A = \begin{bmatrix} \lambda_1 & 0 & \cdot & 0 & 0 \\ 0 & \lambda_2 & \cdot & 0 & 0 \\ \cdot & \cdot & \cdot & \cdot & 0 \\ \cdot & \cdot & \cdot & \lambda_i & \cdot \\ 0 & 0 & \cdot & 0 & \lambda_n \end{bmatrix} \begin{bmatrix} \psi_1 \\ \psi_2 \\ \vdots \\ \psi_i \\ \vdots \\ \psi_n \end{bmatrix} \quad 2.19$$

$$\Psi A = \Lambda \Psi \quad 2.20$$

Vector  $\psi$  is a left eigenvector (Equation 2.18) associated with the eigenvalue  $\lambda$  of the state matrix  $A$ .

Consider Equation (2.9) with zero input (i.e.  $\Delta \mathbf{u} = 0$ ). All the state variables are linearly contributing to the rate of change of each state variable. Therefore, it is vital to isolate and decouple each parameter to identify the most significant variable. In order to decoupling the state variables, new state vector ( $z$ ) is introduced such that,

$$\Delta x = \Phi z \quad 2.21$$

Using the relationships in Equation (2.9), (2.20) and (2.21) it can be proven that,

$$\dot{z} = \Lambda z \quad 2.22$$

Equation (2.22) is the model form of the original state equation (Equation 2.9) with zero input. Since  $\Lambda$  is a diagonal matrix, Equation (2.22) represents set of uncoupled scalar differential equations. The variable  $z$  is defined as a mode or modal variable of the system. From the Equation (2.17) and (2.21) it can be proven that,

$$z = \Psi \Delta x \quad 2.23$$

From Equation (2.21), right eigenvector gives the relative contribution of the each state variable in a particular mode ( $z$ ). In Equation (2.23), left eigenvector identify

the combination of the state variables in a particular mode ( $z$ ). By combining right eigenvectors and left eigenvectors, participation matrix is obtained to identify the relationship between the states and modes of the system more accurately [3] [5].

$$P = [P_1 \ P_2 \ \dots \ P_i \ \dots \ P_n] \quad 2.24$$

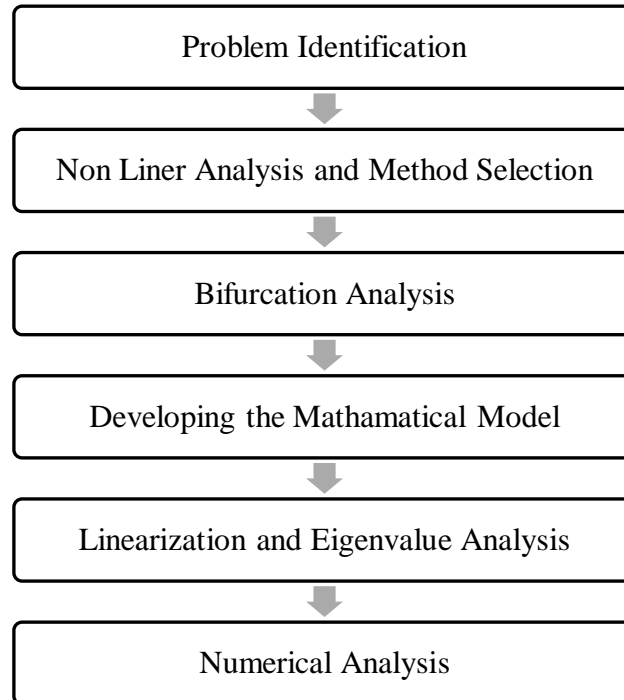
$$P_i = \begin{bmatrix} p_{1i} \\ p_{2i} \\ \cdot \\ p_{ki} \\ \cdot \\ p_{ni} \end{bmatrix} = \begin{bmatrix} \varphi_{1i} \ \psi_{i1} \\ \varphi_{2i} \ \psi_{i2} \\ \cdot \\ \varphi_{ki} \ \psi_{ik} \\ \cdot \\ \varphi_{ni} \ \psi_{n1} \end{bmatrix} \quad 2.25$$

The element  $p_{ki}$  in Equation (2.25) is the participation factor and it measures the relative participation (net) of the  $k^{\text{th}}$  state variable in the  $i^{\text{th}}$  mode in a particular system.

### 3 METHODOLOGY

---

Methodology used in this research can be summarised as follows.



#### 3.1 Problem Identification

Demand for the electricity in Sri Lanka has been increased rapidly during the past few years. Due to the supply limitations power system had to operate closer to its margins to cater the demand continuously. Therefore, it is vital to have a proper understanding of the system stability under the tight loading conditions. In such conditions, nonlinearities become prominent and should consider when defining the stability boundaries of the system. To address this problem, analysis based on nonlinear theories is suggested. Voltage stability of the network is studied and the influence of the system parameters are analysed using selected nonlinear methodology.

#### 3.2 Nonlinear Analysis and Method Selection

Eigenvalue analysis based on linearized systems is a traditional and convenient method used to evaluate stability. However, when applying this method to evaluate the nonlinear system, the detailed aspect of the nonlinear behaviour cannot be obtained. Therefore, it is vital to use nonlinear methods to get a proper understanding of the system. Bifurcation method is selected after evaluating other nonlinear

approaches such as dynamic phasor, reduced order modelling and scholastic modelling [18] [19] [20].

### 3.3 Bifurcation Analysis

A continuous dynamic system can be well explained using a set of Ordinary Differential Equations (ODEs). These equations mostly contain parameters along with system variables. Small change to these parameters can cause sudden variations in the system behaviour. Bifurcation analysis deals with identifying these branching phenomena of the system qualitatively under the influence of critical parameter (bifurcation parameter).

### 3.4 Developing the Mathematical Model

A mathematical model is developed incorporating all the major elements of the system. To represent the synchronous generator more accurately six variable model is used along with the exciter model. This helps to identify the influence of the power plant to the network changes more accurately. System modelling is given in Chapter 4.

### 3.5 Linearization and Eigenvalue Analysis

Set of ODEs linearized around the equilibrium point and obtained a system matrix. To evaluate the voltage stability of the network, reactive power of the load bus is selected as a variable parameter. The Analysis is done for both intact and contingency conditions to identify system behaviour under the different operating situations. Using the derived system matrix eigenvalues were calculated. Eigenvalue movement was then analysed with the change in the selected parameter and the stability was explained using the bifurcation theory.

### 3.6 Numerical Analysis

New functions were developed using MATLAB to solve the ODEs numerically and obtain load flow calculation (Appendix C). Bifurcation diagram is obtained and results from eigenvalue analysis were compared with bifurcation outcomes. Following steps were involved in the computation.

- Calculate the  $Y_{bus}$  matrix for the selected condition
- Read the given input related to the system element
- Perform load flow calculation and derive equilibrium condition
- Solve the system numerically using derived equilibrium data
- Evaluate for different perturbations

## 4 MODELLING THE SYSTEM

---

### 4.1 Introduction

As discussed earlier, the power system is a nonlinear, multivariable dynamic system comprise of different elements. Modelling the system to represent actual behaviour is vital to carry out proper analysis. Main components of the system can be divided into four sections and detailed discussions on modelling these elements are presented in the following sections.

### 4.2 Synchronous Generator Model

As discussed in Section 1.1, Lakvijaya power station has three, two pole, cylindrical rotor synchronous generators each rated at 353 MVA. The generator output voltage is 20 kV, which is then stepped up to 220 kV. It is driven by a steam turbine directly coupled through a single shaft. Sixth order mathematical model is used to model the generator, which represents the dynamic behaviour of the generator rotor, field winding and the damper windings. Damper windings consist with one winding along the d axis and two windings along the q axis. Parameters of Equations (4.1) to (4.6) were configured based on [5], and transient and sub transient characteristics are also considered.

$$\Delta \dot{w}_r = \frac{1}{2H} [P_m - P_e - k_D \Delta w_r] \quad 4.1$$

$$\dot{\delta} = w_0 \Delta w_r \quad 4.2$$

$$\dot{\psi}_{fd} = \frac{w_0 R_{fd}}{L_{adu}} E_{fd} - \frac{w_0 R_{fd}}{L_{fd}} \psi_{fd} + \frac{w_0 R_{fd}}{L_{fd}} [L''_{ads} (-i_d + \frac{\psi_{fd}}{L_{fd}} + \frac{\psi_{1d}}{L_{1d}})] \quad 4.3$$

$$\dot{\psi}_{1d} = w_0 [-\frac{R_{1d}}{L_{1d}} \psi_{1d} - \frac{R_{1d}}{L_{1d}} L''_{ads} (-i_d + \frac{\psi_{fd}}{L_{fd}} + \frac{\psi_{1d}}{L_{1d}})] \quad 4.4$$

$$\dot{\psi}_{1q} = w_0 [-\frac{R_{1q}}{L_{1q}} \psi_{1q} + \frac{R_{1q}}{L_{1q}} L''_{aqs} (-i_q + \frac{\psi_{1q}}{L_{1q}} + \frac{\psi_{2q}}{L_{2q}})] \quad 4.5$$

$$\dot{\psi}_{2q} = w_0 [-\frac{R_{2q}}{L_{2q}} \psi_{2q} + \frac{R_{2q}}{L_{2q}} L''_{aqs} (-i_q + \frac{\psi_{1q}}{L_{1q}} + \frac{\psi_{2q}}{L_{2q}})] \quad 4.6$$

Where,

$\Delta w_r$  = Rotor speed deviation

$\delta$  = Rotor angle

$\psi_{fd}$  = Field winding flux

$\psi_{1d}$  = Direct axis damper winding flux

$\psi_{1q}, \psi_{2q}$  = Quadrature axis damper winding flux

### 4.3 Exciter Model

Thyristor controlled static exciter is used in power plant to generate required DC voltage to excite the synchronous generator. Excitation voltage and current of the exciter are 365 V and 2642 A respectively. A separate transformer, connected to the output terminal of the generator, is used to energize the exciter. IEEE AC4 excitation system model, as shown in Figure 4.1, was selected [21].

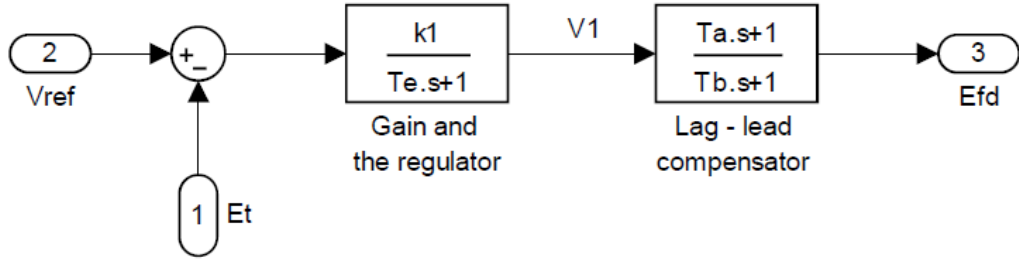


Figure 4.1 : IEEE AC4 Exciter Model

$$\dot{V}_1 = \frac{1}{T_e} [-V_1 + k_1(V_{ref} - E_t)] \quad 4.7$$

$$\dot{E}_{fd} = \frac{1}{T_b} [-E_{fd} + V_1 \left(1 - \frac{T_a}{T_e}\right) + \frac{k_1 T_a}{T_e} (V_{ref} - E_t)] \quad 4.8$$

Where,

$E_{fd}$  = Field Voltage

$V_{ref}$  = Reference Voltage

$E_t$  = Terminal Voltage

### 4.4 Load Model

The power system, in general, is a complex structure comprised of generators, transmission networks, distribution networks, and loads. Stable operation of a power system solely depends on the ability to match generation with loads on the system. When analysing the power system, distribution levels are generally not considered directly but replaced by equivalent loads referred as composite loads [3]. These

composite loads can be classified into two categories: static and dynamic loads. Generally, a static representation is used in load flow studies [13]. However, for the small signal and transient studies, application of the dynamic load model is vital. Following dynamic load model is used in this study.

$$P = P_0 + P_1 + k_{pw} \dot{\delta} + k_{pv}(V + TV) \quad 4.9$$

$$Q = Q_0 + Q_1 + k_{qw} \dot{\delta} + k_{qv}V + k_{qv2}V^2 \quad 4.10$$

Where,

$V$  = Bus voltage

$\delta$  = Rotor angle

$P_0, Q_0$  = Static active and reactive component of the dynamic load

$P_1, Q_1$  = Active and reactive component of the static load

$P, Q$  = Active and reactive component of the composite load

#### 4.5 Network model

The Lakvijaya power plant is connected to the national grid via New Anuradhapura (NA) and New Chilaw (NC) 220 kV double circuit lines having a length of 100 km and 74 km respectively. NA 220 kV bus is connected to the New Habarana (NH) via 220 kV, 50 km long double circuit line. NH bus is connected to NC 220 kV bus through Veyanagoda substation forming a 220 kV ring network (Figure 4.2).

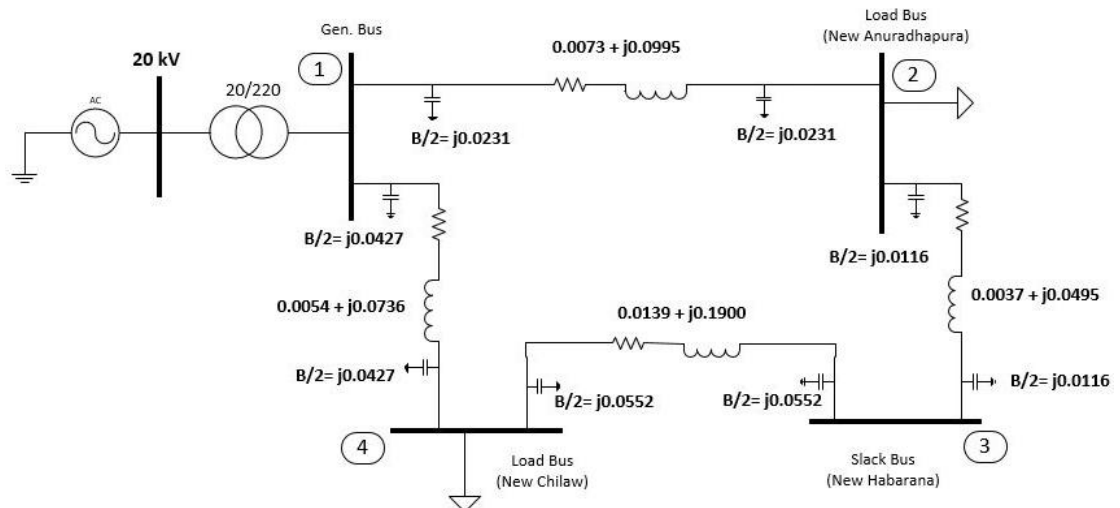


Figure 4.2 : Network in Intact Condition

Since the Kothmale 220 kV bus is connected to the NH substation, it is taken as a swing bus for the power flow calculation. NA and NC buses were considered as load buses and connected to the dynamic loads respectively [22].

#### 4.6 System Configuration

The generator of the system was modelled using the sixth order model as explained in Chapter 4. Detailed modelling of the generator (Equation A.1 to A.24) and dynamic data used are given in Appendix A.1. The detailed exciter modelling and parameter values are illustrated in Appendix A.2. Figure 4.2 presents the network model used in this study and details are given in Appendix A.3. For the analysis, bus 4 is considered as the swing bus. Composite load model is used to represent the loading of the buses [13] [23]. Load of each bus was analysed and values for the gains were calculated using the 220 kV bus (both NA and NC) data in Appendix B.

## 5 RESULTS AND ANALYSIS

Linearised model was used to obtain the system matrix of the system. Then eigenvalues were calculated and the movement of the critical eigenvalues were analysed.

### 5.1 Test System in Intact Condition

The test system in the Figure 4.2 consists of 12 state variables and system matrix was obtained from linearized equations in Appendix A.3 for the intact condition. The nominal operating point of the power system under consideration was calculated from power flow equations and stability was evaluated using eigenvalue analysis. Then, the reactive load at the bus 4 (Figure 4.2) increased to simulate the stressed operating condition.

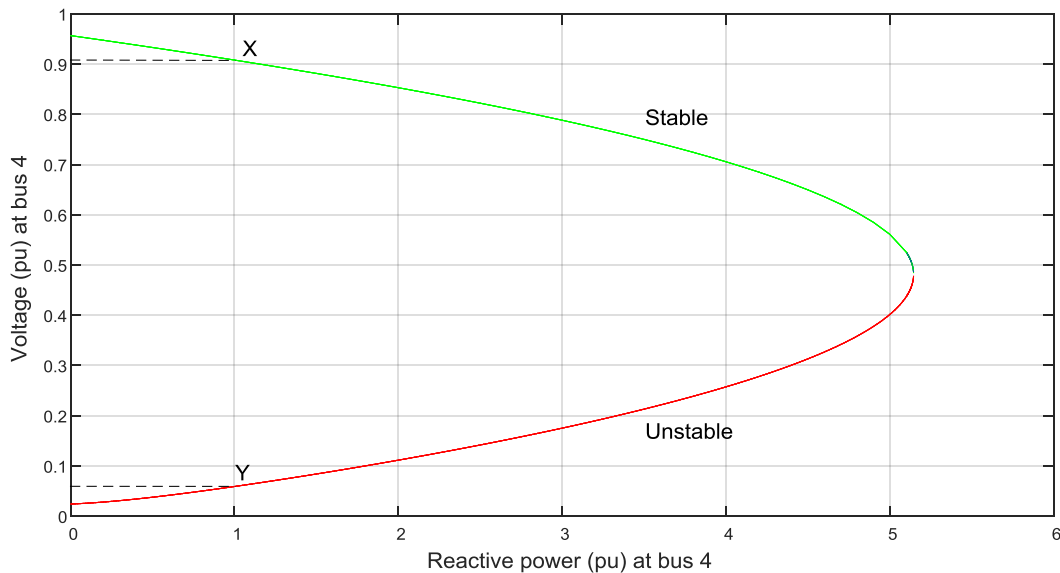


Figure 5.1 : Reactive power Vs Voltage

First, the dynamic behaviour of the intact system is analysed varying the reactive power at the bus 4. When the reactive power increased, the voltage at bus 4 gradually decreases (or increases). After significant increment of reactive power, saddle node bifurcation happened and there is no possible operating point beyond this loading point. In between this saddle point and nominal loading value, there are two possible operating conditions (Figure 5.1). These two conditions were analysed using the eigenvalues to identify the stability.

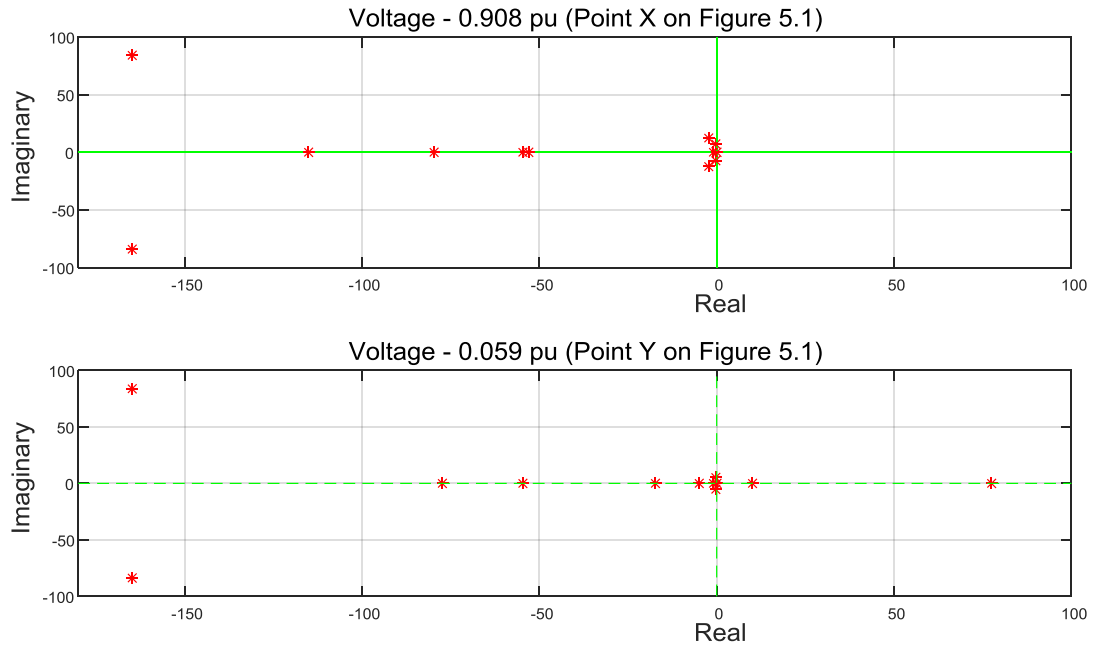


Figure 5.2 : Eigen Values

Figure 5.2 shows the eigenvalues related to the two possible operating conditions at the reactive power of 1 pu. All the eigenvalues at 0.908 pu voltage, were at the left half plane of the real axis. Whereas some eigenvalues of the other solution, i.e. 0.059 pu, were at the right half plane of the real axis. Therefore, only the 0.908 pu voltage level is the stable solution. When reactive loading at the bus increases further voltage begins to decrease till there is no equilibrium point.

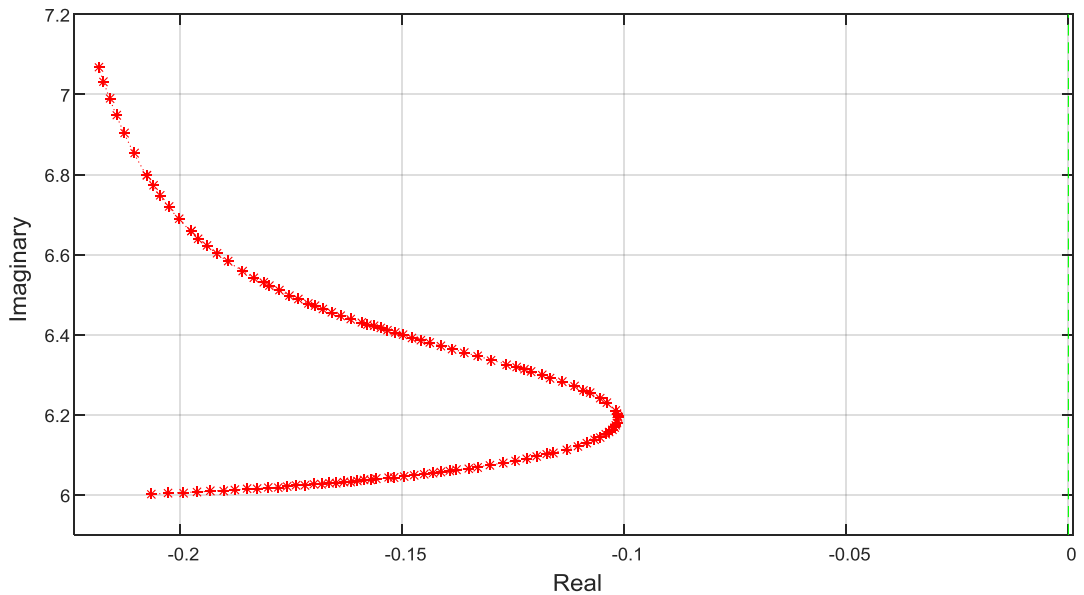


Figure 5.3 : Eigenvalue Movement in Intact Network

Further, the eigenvalue movement was analysed by varying the reactive power at the load bus. The movement of the relevant eigenvalues as the loading is increased is shown in Figure 5.3. Only the stable voltage solution is considered to identify the eigenvalue movement when increasing the loading of the bus. All the eigenvalues till the saddle node point were in left half resulting stable operating region. Results indicate that under the intact condition of the system it is going to be stable for the reactive loading till the saddle node point.

## 5.2 Test System in Contingency Condition

Then the system is analysed for a contingency situation as shown in Figure 5.4.

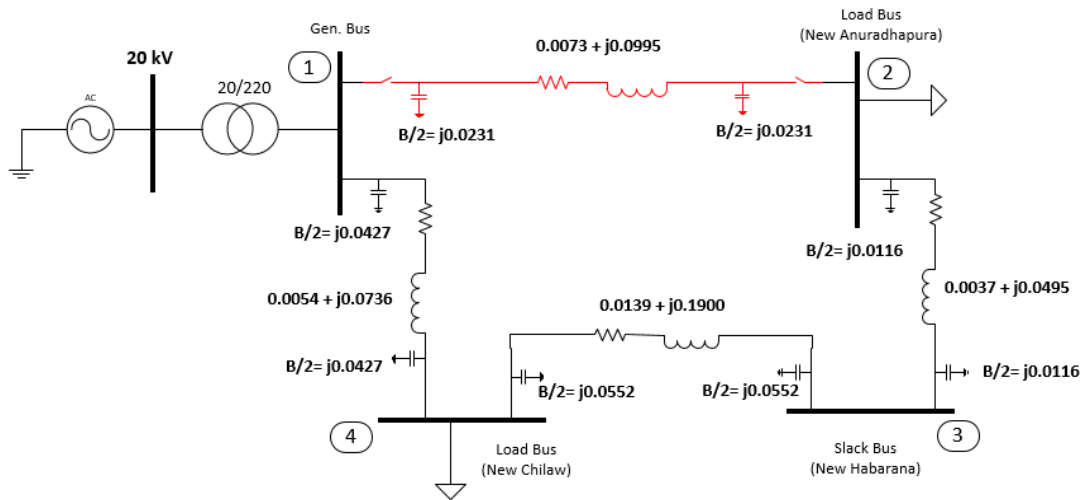


Figure 5.4 : One Line Outage – New Anuradhapura

New Anuradhapura double circuit line outage was considered and all the other parameters were kept as in intact condition. Eigenvalue movements related to the stable solution was analysed with the increase in reactive power loading at bus 4.

It was observed that all the eigenvalues move toward the right half plane when increasing the parameter. At the reactive loading of 4.9169 pu, a pair of eigenvalues crosses the real axis at  $(0.0 \pm 3.5381i)$  as shown in Figure 5.5 (eigenvalue having positive imaginary part is used from the pair of critical eigenvalue). Loading was further increased and at 5.12200 pu of reactive loading, critical eigenvalues pair again crosses the real axis at  $(0.0 \pm 1.4445i)$ , and moves back to the left half plane.

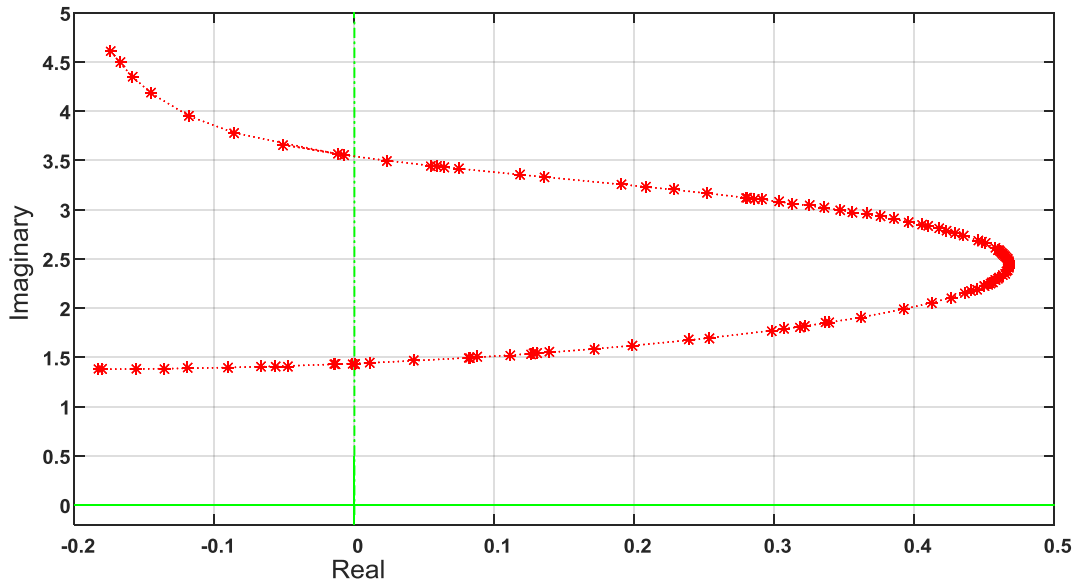


Figure 5.5 : Critical Eigenvalue Movement in Contingency Condition

Figure 5.6 shows the voltage profile when increasing the reactive load at bus 4 under the contingency situation. According to the stability criterion based on eigenvalues, system behaviour can be explained as follows: Before system reach point A, all twelve eigenvalues were in left half plane and system is well stable for small disturbances. With the loading pair of eigenvalue crosses the real axis at point A leading to voltage instability.

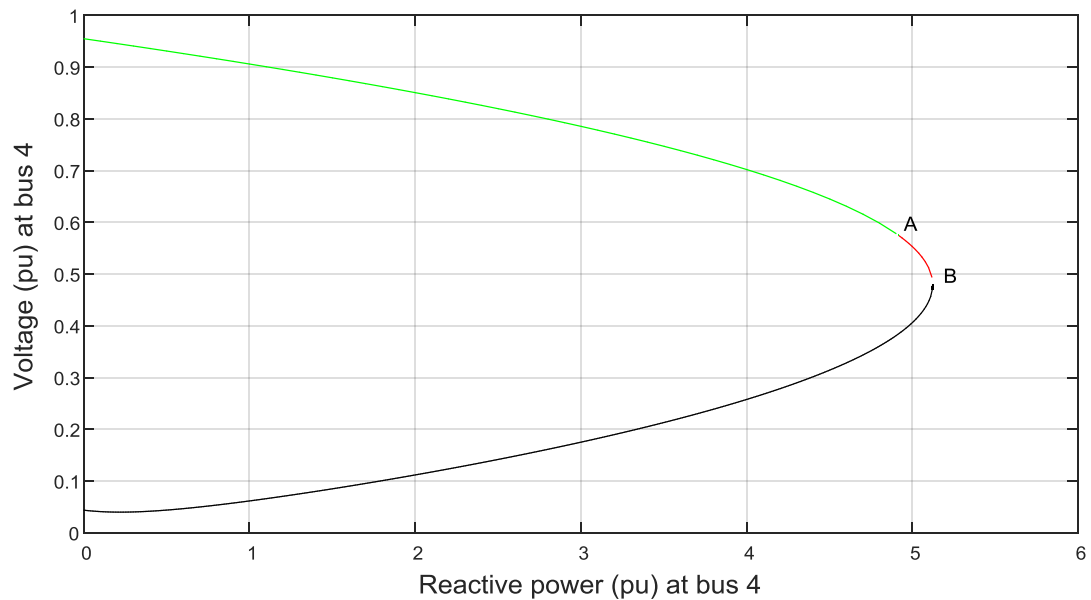


Figure 5.6 : Reactive Power Vs Voltage

Therefore, between the point **A** and **B**, system experiences voltage instability and after point **B**, system becomes stable again till the system losses equilibrium at the saddle node.

### 5.3 Bifurcation Analysis

First, consider the intact condition. As explained earlier there are two equilibriums for the system. One is stable i.e. all the eigenvalues are in the left half plane while other equilibrium point is unstable i.e. one or more pair of eigenvalues are in the right half plane. When all the eigenvalues are in the stable region, the trajectory behaviour around the singular point will be a stable node. The unstable equilibrium point is having a saddle node trajectory (as discussed in chapter 2). When loading increases these two trajectories collide with each other and saddle node bifurcation will happen. With the saddle node bifurcation, the voltage magnitude of the load bus drops suddenly in a very short period of time resulting a voltage collapse. After this point system has no equilibrium condition.

System behaviour changed drastically with the outage of NA line. In this condition, the saddle node point can be identified as in intact situation. Eigenvalue analysis shows that the system experience instability before the saddle node point. Let's discuss this behaviour using bifurcation theories.

In the nominal loading conditions, all the eigenvalues are in the stable region (left half plane). As discussed earlier, when loading increases real part of the pair of eigenvalues crosses the real axis. At this point, the following conditions are satisfied: [17] [9]

- At the point of crossing, all the state values satisfy the system equations. i.e. the point under consideration is an equilibrium point  

$$F(x_0, \alpha_0) = 0$$
- System matrix of the liberalised system has a simple pair of purely imaginary eigenvalues. ( $0.0 \pm 3.5381i$  and  $0.0 \pm 1.4445i$ )  

$$\lambda_{1,2} = \pm wi, w > 0$$
  
 In this system eigenvalue at the crossing point is  $0.0 \pm 3.5381i$
- The critical eigenvalue should cross the real axis with non zero speed  

$$\frac{d(Re(\lambda))}{d\alpha} \neq 0$$

Therefore, at the point **A** and **B** conditions for the Hopf bifurcation are satisfied. As the loading increases from the nominal value, an unstable periodic orbit and stable equilibrium point join together at point **A** leaving an unstable equilibrium point. When increasing the reactive load, all the eigenvalues are in the stable region till the point **A**. That means the system is in equilibrium and stable at the point **A**. If the load

is increased further, the system moves to an asymptotically stable region where the boundary is defined by an unstable periodic orbit.

At the point **B**, again the pair of eigenvalues crosses the real axis. As the loading increases, a stable periodic orbit and an unstable equilibrium point join together at point **B**, leaving a stable equilibrium point. Between the point **A** and **B**, some eigenvalues are in the right half plane. This means that there is no stable equilibrium point. However, from the bifurcation theories, there is a stable periodic orbit creating a uniformly asymptotically stable region.

#### 5.4 Results Validation

The nonlinear system was then analysed using a numerical method with the help of MATLAB (R2015a) to validate the system behaviour. All the system equations (12 nos) were solved for the different loading conditions to obtain initial values to be used in numerical analysis. A MATLAB function was developed to compute the initial conditions for all the system equation with the varying loading conditions. The bifurcation diagram was obtained for both supercritical Hopf and subcritical Hopf by analysing the system behaviour for a small disturbance under the bifurcation conditions.

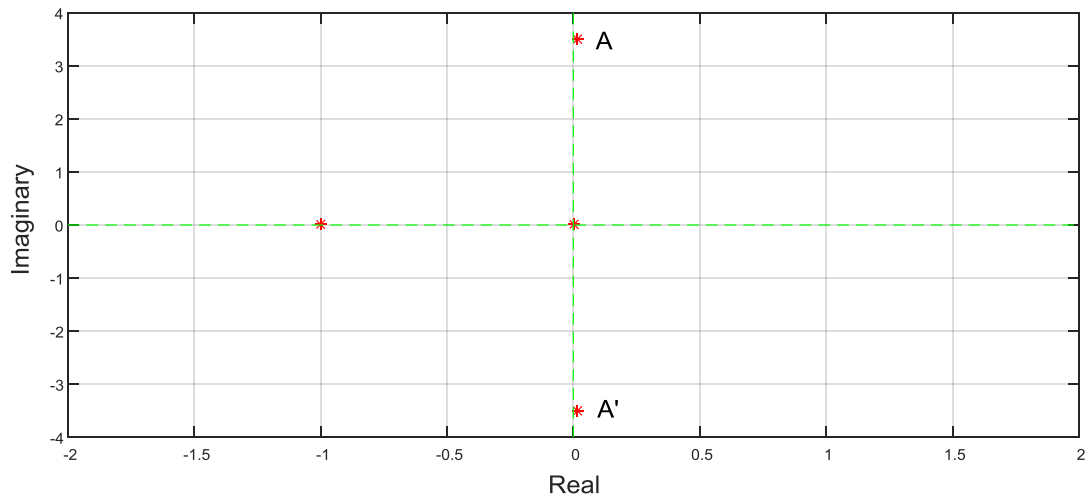


Figure 5.7 : Critical Eigenvalues at Subcritical Hopf

Reactive loading at the bus 4 was selected as 4.95 pu to analyse the subcritical bifurcation. As shown in Figure 5.7, at this loading condition, real parts of the pair of complex eigenvalues are in right half plane (point **A** and **A'** are  $0.0172 \pm 3.5088i$ ). As discussed in the Section 2.10 the system should experience subcritical bifurcation. By solving the system equations using numerical methods equilibrium point is obtained. The equilibrium parameters for the state variable under consideration for this discussion at that loading condition were  $V_4 = 0.5668$  pu and  $\delta = 0.13652$  pu. Then, the small voltage disturbance of 0.0001 pu was given to the system to observe

the behaviour. As shown in Figure 5.8 system undergoes some oscillations and settles after around 10 s at a stable position. Participation factor analysis [5] [24] was used to determine which state variables are contributing to the occurrence of bifurcation.

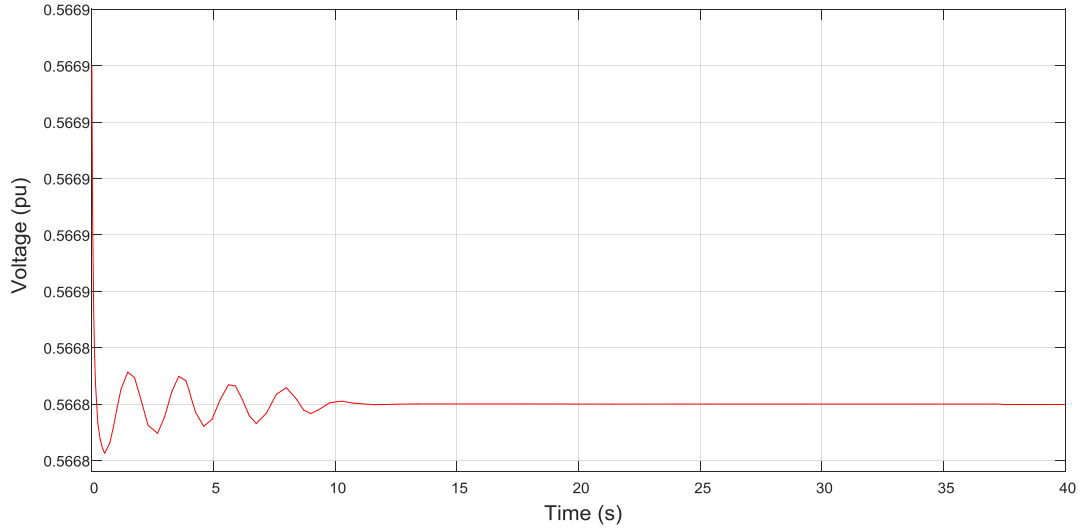


Figure 5.8 : Subcritical Hopf – Stable System

Participation factor analysis reveals that near the singular point, the state variables, rotor angle ( $\delta$ ) and rotor speed deviation ( $\Delta\omega_r$ ) has the strongest influence for the occurrence of bifurcation (Table 5.2). Figure 5.9 shows the bifurcation diagram of rotor angle versus voltage at bus 4. Point **A** represents the voltage disturbance given to the system. After some oscillations, system settled at point **B**, which is the original stable point.

Now the system is analysed by giving disturbance of 0.01 pu for the voltage such that it will be overthrown to the outside of the unstable limit cycle. The equilibrium point is the same as in previous. As shown in Figure 5.10, with the disturbance, system starts to oscillate and the magnitude of the oscillation increases gradually leading to the system instability. The system behaviour analysed considering rotor angle and bus voltage as in Figure 5.11. The disturbance of 0.01 pu, forced the trajectory to shift outside the limit cycle (point **A** in Figure 5.11). Then the system experience an oscillation, which is having an increasing magnitude indefinitely (point **B** in Figure 5.11), and the system experienced instability leading to the voltage collapse of the bus.

The strong influence from the rotor angle ( $\delta$ ) and rotor speed deviation ( $\Delta\omega_r$ ) to the occurrence of the Hopf bifurcation and subsequent instability in the system reveals that it can be associated to an angle instability (Table 5.2) [7].

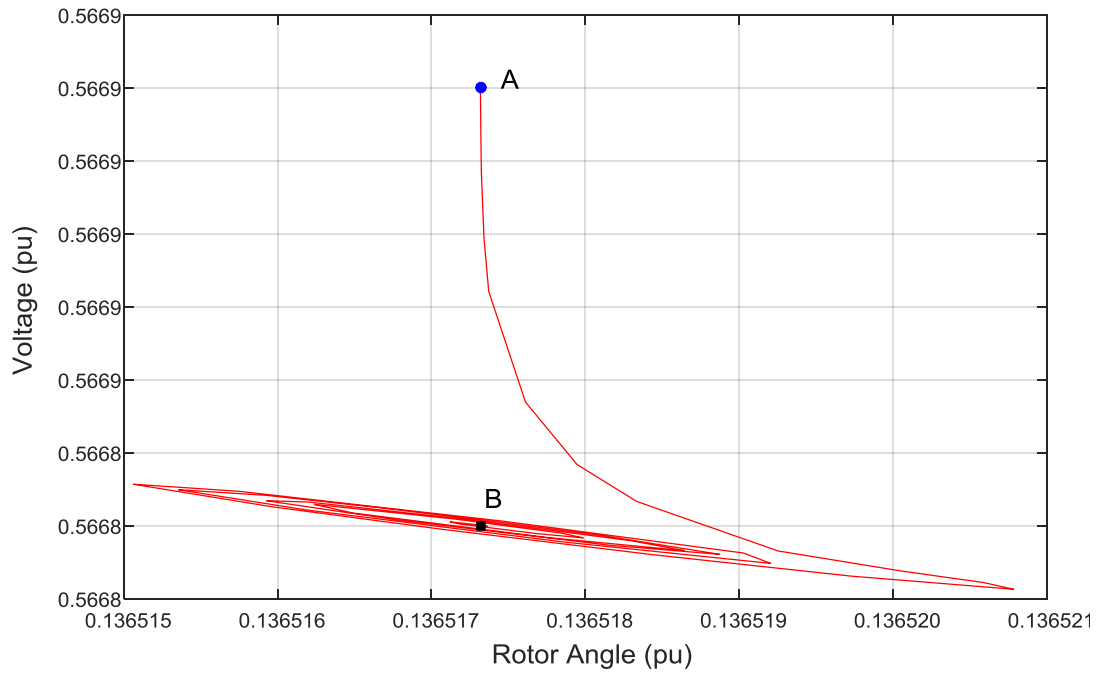


Figure 5.9 : Rotor Angle Vs Voltage

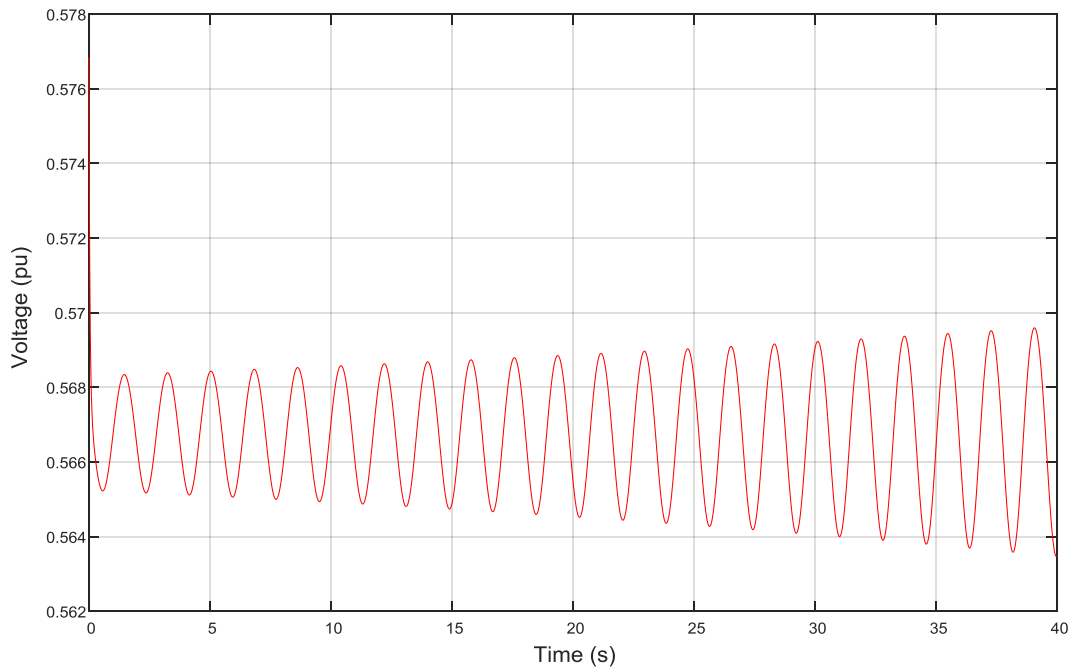


Figure 5.10 : Subcritical Hopf – Unstable System

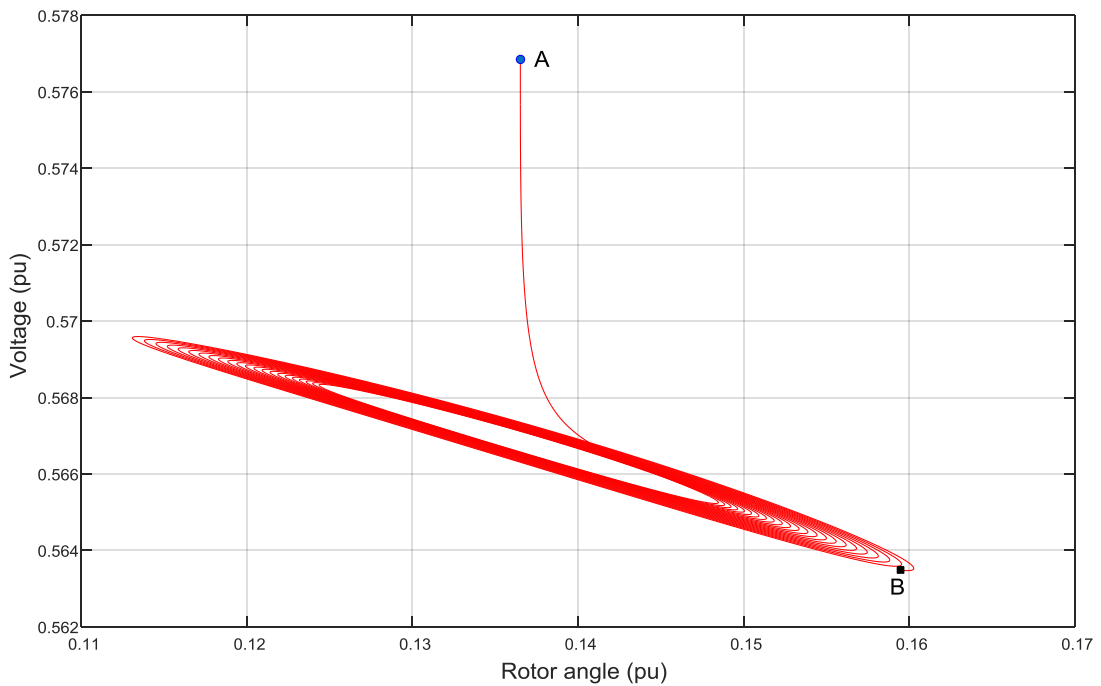


Figure 5.11 : Subcritical Hopf – Unstable System

Supercritical bifurcation was analysed considering a reactive load of 5.122 pu at bus 4. The eigenvalues at this reactive loading were shown in Figure 5.12 (point  $A$  and  $A'$  are  $0.1347 \pm 1.5458i$ ). In supercritical Hopf, there is a stable limit cycle exists around the unstable equilibrium point. As discussed in Chapter 2, at the supercritical Hopf, a stable limit cycle exists around the unstable equilibrium point. Equilibrium value for the voltage at this loading condition is 0.4808 pu. When the system undergoes a disturbance, the voltage starts to oscillate. Disturbance of 0.001 pu is given to the voltage at the bus and response is observed (Figure 5.13). With the disturbance, voltage oscillation was observed. The oscillation sustained over the time and the system is uniformly asymptotically stable. Using participation factor analysis it can be identified that the rotor angle ( $\delta$ ) and Rotor speed deviation ( $\Delta\omega_r$ ) has the strongest influence over the bifurcation at this system conditions. Figure 5.14 shows the variation of the bus voltage with the rotor angle for a voltage disturbance of 0.001 pu. With this disturbance voltage shifted outside the limit cycle (point  $A$  in Figure 5.14). The magnitude of the oscillation gradually reduced and settled in a stable limit cycle (point  $B$  in Figure 5.14).

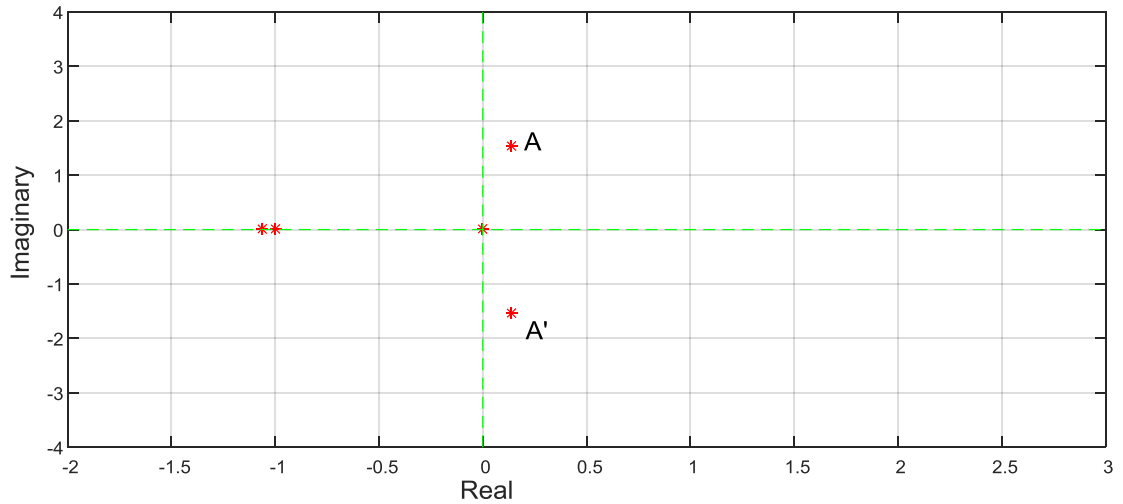


Figure 5.12 : Critical Eigenvalues at Supercritical Hopf

As illustrate in Figure 5.15, with the small perturbation of 0.0005 pu, the voltage remains inside the limit cycle. In observing the voltage response shown in Figure 5.16, the system experience an oscillation which is having an increasing magnitude (point *A* corresponding to Figure 5.15), and then settle in the stable limit cycle (point *B* corresponding to Figure 5.15).

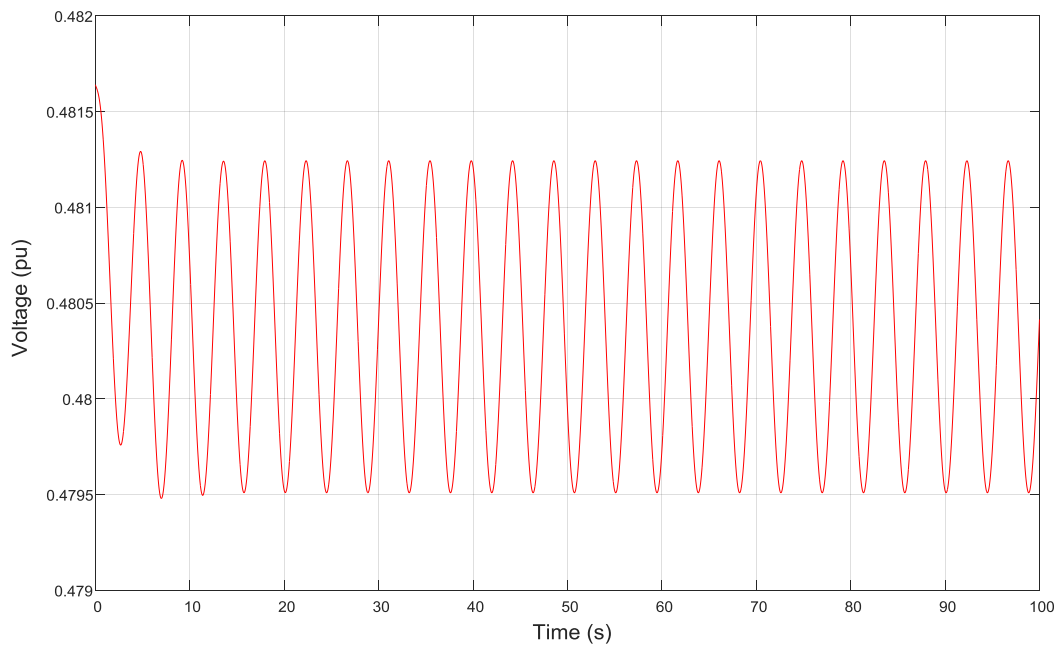


Figure 5.13 : Supercritical Hopf – Outside the Limit Cycle

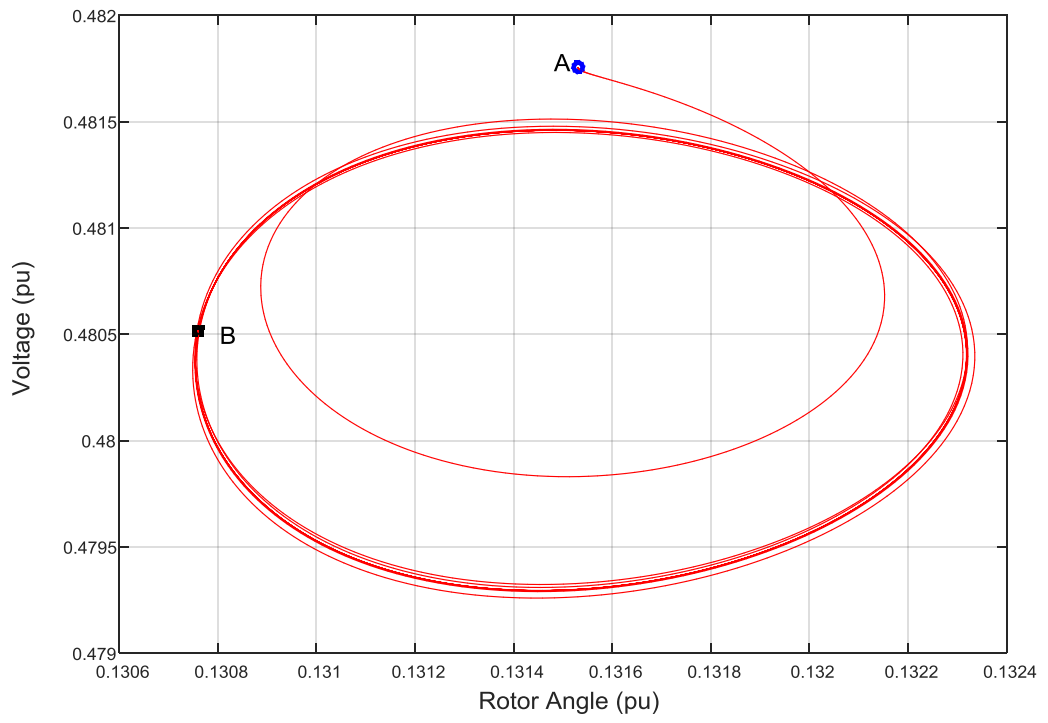


Figure 5.14 : Rotor Angle Vs Voltage – Outside the Limit Cycle

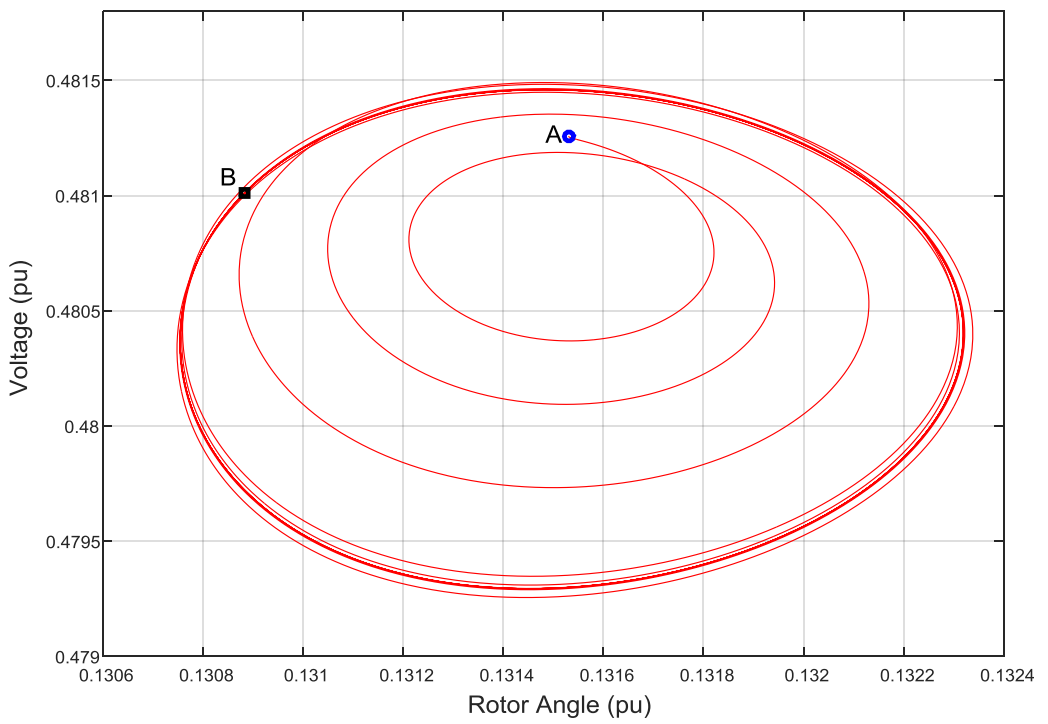


Figure 5.15 : Rotor Angle Vs Voltage – Inside the Limit Cycle

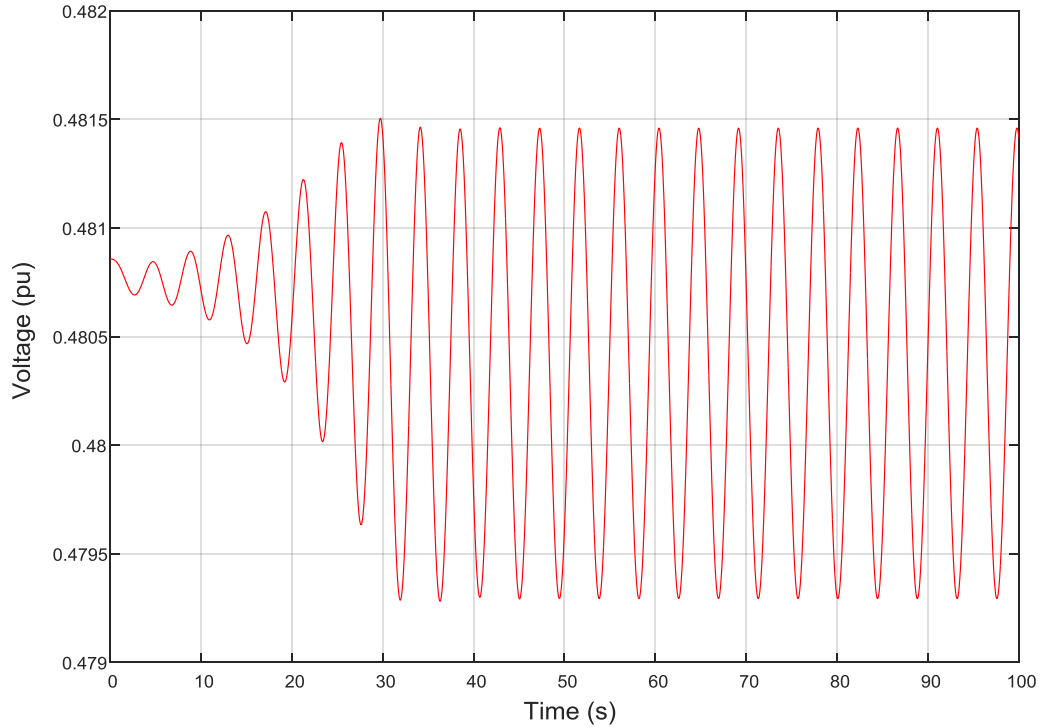


Figure 5.16 : Supercritical Hopf – Inside the Limit Cycle

### 5.5 Participation Factor Analysis

With reference to Figure 5.4, when one line (NA) is out in the system a pair of complex eigenvalues is crossing the real axis with the change in reactive loading resulting Hopf bifurcation. This pair of eigenvalues is identified as critical eigenvalues, which are associated with critical mode. Then the state participation factors were calculated corresponding to the critical eigenvalues (modes) to identify the state variables that are responsible for the oscillatory behaviour of the system. Participation factors calculated at subcritical and supercritical Hopf bifurcations are illustrated in Table 5.1 and Table 5.2 respectively.

Table 5.1 : Subcritical Hopf – Largest Participation Factors

State Variable	Participation Factor
Rotor angle	0.4615
Rotor speed deviation	0.4584
Voltage at bus 4	0.2297
Voltage angle of bus 4	0.1766

Table 5.2 : Supercritical Hopf – Largest Participation Factors

State Variable	Participation Factor
Rotor angle	0.4875
Rotor speed deviation	0.4870
Voltage at bus 4	0.0709
Voltage angle of bus 4	0.0481

Four state variables were identified, which had the largest influence for the bifurcation in both situations. As given in Table 5.1, Rotor angle ( $\delta$ ) is the most influencing state variable for subcritical Hopf bifurcation of the system followed closely by the Rotor speed deviation ( $\Delta\omega_r$ ) having participation factors of 0.4615 and 0.4584 respectively. As depicted by Table 5.2, participation factor analysis for the supercritical Hopf shows that same state variables i.e. Rotor angle ( $\delta$ ) and Rotor speed deviation ( $\Delta\omega_r$ ) influence the bifurcation mostly.

## 6 CONCLUSIONS

---

### 6.1 Conclusions

When the system operates under the normal operating conditions it is possible to use linearized methods and analyse the behaviour correctly. However, this study shows that under the stressed operating conditions linearized analysis is not giving the proper behaviour of the system. The recent advancements of bifurcation theories have made it possible to analyse power systems more accurately and qualitatively compared to other available nonlinear analysis methods.

In this research Hopf bifurcation analysis was carried out to study the system behaviour in a small power system having a large generator connected. Sri Lankan power system having 900 MW coal power plant (Lakvijaya) was considered as a case study. The study reveals the existence of stable and unstable limit cycle when the system experienced stressed loading conditions. Reactive power demand at the load bus was used as a parameter under consideration and identified the critical values that lead to dynamic voltage stability. This information can be incorporated in developing protection schemes in the transmission network. Further, participation factor analysis shows that rotor angle is the most influencing factor for the Hopf bifurcation in the system considered. This reveals the importance of Power System Stabilizer (PSS) being installed at the Lakvijaya power plant, and it is highly advisable to correctly tune the gain values of the PSS considering network contingencies.

### 6.2 Future Directions

In order to get a proper understanding of the power system considering the nonlinear behaviour under the contingency conditions, following areas still need to be addressed:

1. Include control devices such as PSS, FACTS to the analysis. It is then possible to identify the correct placement of such devices.
2. Extend the study incorporating other types of bifurcation phenomena such as zero Hopf and double parameter analysis. Further, to get a proper understanding of the system behaviour, it is essential to analyse complete power system of Sri Lanka using the proposed methods
3. Develop indices to identify the bifurcation in the power system. This helps to detect and predict the stability problems related to power system more conveniently.

## References

---

- [1] “Statistical Digest,” Ceylon Electricity Board, 2017.
- [2] “Performance 2017 & Programme for 2018,” Ministry of Power and Renewable Energy, Colombo, 2017.
- [3] J. Machowski, J. W. Bialek and J. R. Bumby, *Power System Dynamics - Stability and Control*, West Sussex: John Wiley & Sons, Ltd, 2008.
- [4] A. H. Nayfeh and B. Balachandran, *Applied Nonlinear Dynamics Analytical, Computational and Experimental Methods*, Weinheim: WILEY-VCH Verlag GmbH & Co, 2004.
- [5] P. Kundur, *Power Systems Stability and Control*, New York: McGraw Hill Inc, 1993.
- [6] M. K. M. Rabby, A. H. Chowdhury, M. A. Azamand and M. A. Towfiq, “Bifurcation analysis to identify voltage collapse in bangladesh power system,” in *2013 International Conference on Informatics, Electronics and Vision (ICIEV)*, Dhaka, 2013.
- [7] P. Kundur, J. Paserba, V. Ajarapu, G. Andersson, A. Bose, C. Canizares, N. Hatziargyriou, D. Hill, A. Stankovic, C. Taylor and T. Van Cutsem, “Definition and classification of power system stability IEEE/CIGRE joint task force on stability terms and definitions,” *IEEE Transactions on Power Systems*, vol. 19, no. 3, pp. 1387 - 1401, 2004.
- [8] L. Y. Taylor and S.-M. H. , “Transmission voltage recovery following a fault event in the Metro Atlanta area,” in *2000 Power Engineering Society Summer Meeting*, Seattle, WA, USA, 2000.
- [9] N. Mithulananthan and S. C. Srivastava, “Investigation of a voltage collapse incident in Sri Lankan power system network,” in *Proceedings of EMPD '98. 1998 International Conference on Energy Management and Power Delivery*, Singapore, 1998.
- [10] C. D. Vournas, G. A. Manos, J. Kabouris and T. Van Cutsem, “Analysis of a voltage instability incident in the Greek power system,” in *2000 IEEE Power Engineering Society Winter Meeting. Conference Proceedings*, Singapore, 2000.
- [11] R. Seydel, *Practical Bifurcation and Stability Analysis*, New York: Springer, 2010.

- [12] Y. A. Kuznetsov, *Element of Applied Bifurcation Theory*, vol. 112, New York: Springer, 1998.
- [13] G. Revel, D. M. Alonso and J. L. Moiola, "Power Systems Bifurcation Theory Applied to the Analysis of Power systems," *Revista De La Union Matematica Argentina* , vol. 49, no. 1, pp. 1-14, 2008.
- [14] G. Revel, A. E. León, D. M. Alonso and J. L. Moiola, "Bifurcation Analysis on a Multimachine Power System Model," *IEEE Transactions on Circuits and Systems I*, vol. 57, no. 4, pp. 937 - 949, 2009.
- [15] J. Li, X. Zhou and G. Dong, "Hopf bifurcation analysis on dynamic voltage stability of wind power systems with SVC," in *IEEE International Conference on Mechatronics and Automation*, Tianjin, 2014.
- [16] M. Watanabe, Y. Mitani and K. Tsuji, "Evaluation of a Power System Stable Region Based on Hopf Bifurcation Theory," *IEEJ Transactions on Power and Energy*, vol. 142, no. 1, pp. 174 - 180, 2003.
- [17] M. Jazaeri and M. Khatibi, "A Study on Hopf Bifurcations for Power System Stability Analysis," in *2008 IEEE Canada Electric Power Conference*, Vancouver, 2008.
- [18] K. Abojlala, D. Holliday and L. Xu, "Transient analysis of an interline dynamic voltage restorer using dynamic phasor representation," in *2016 IEEE 17th Workshop on Control and Modeling for Power Electronics (COMPEL)*, Trondheim, Norway, 2016.
- [19] S. Dasgupta, M. Paramasivam and U. Vaidya, "PMU-based model-free approach for short term voltage stability monitoring," in *2012 IEEE Power and Energy Society General Meeting*, San Diego, CA, USA, 2012.
- [20] J. C. Lopez, J. Contreras, J. I. Munoz and J. Mantovani, "A Multi-Stage Stochastic Non-Linear Model for Reactive Power Planning Under Contingencies," *IEEE Transactions on Power Systems* , vol. 28, no. 2, pp. 1503 - 1514, 2013.
- [21] "Excitation System Models for Power System Stability Studies," *IEEE Transactions on Power Apparatus and Systems*, Vols. PAS-100, no. 2, pp. 494 - 509, February 1981.
- [22] "Long Term Transmission Development Plan 2013-2022," Ceylon Electricity Board, Colombo, 2013.

- [23] H. Renmu, M. Jin and D. Hill, "Composite load modeling via measurement approach," *IEEE Transactions on Power Systems*, vol. 21, no. No 2, pp. 663-672, May 2006.
- [24] D. Aik and G. Andersson, "Use of participation factors in modal voltage stability analysis of multi-infeed HVDC systems," *IEEE Transactions on Power Delivery*, vol. 13, no. 1, pp. 203 - 211, January 1998.

## Appendix - A: System Modelling

This appendix provides a detailed mathematical description of the system model used in this thesis. Furthermore, this contained data used in different models including synchronous generator, exciter, load model and the network.

### A.1 Synchronous Generator Model

Test system is comprised of twelve state variables and generator modelled using six variables.

$$\Delta \dot{w}_r = \frac{1}{2H} [P_m - P_e - k_D \Delta w_r] \quad \text{A.1}$$

$$\dot{\delta} = w_0 \Delta w_r \quad \text{A.2}$$

$$\dot{\psi}_{fd} = \frac{w_0 R_{fd}}{L_{adu}} E_{fd} - \frac{w_0 R_{fd}}{L_{fd}} \psi_{fd} + \frac{w_0 R_{fd}}{L_{fd}} [L''_{ads} (-i_d + \frac{\psi_{fd}}{L_{fd}} + \frac{\psi_{1d}}{L_{1d}})] \quad \text{A.3}$$

$$\dot{\psi}_{1d} = w_0 [-\frac{R_{1d}}{L_{1d}} \psi_{1d} - \frac{R_{1d}}{L_{1d}} L''_{ads} (-i_d + \frac{\psi_{fd}}{L_{fd}} + \frac{\psi_{1d}}{L_{1d}})] \quad \text{A.4}$$

$$\dot{\psi}_{1q} = w_0 [-\frac{R_{1q}}{L_{1q}} \psi_{1q} + \frac{R_{1q}}{L_{1q}} L''_{aqs} (-i_q + \frac{\psi_{1q}}{L_{1q}} + \frac{\psi_{2q}}{L_{2q}})] \quad \text{A.5}$$

$$\dot{\psi}_{2q} = w_0 [-\frac{R_{2q}}{L_{2q}} \psi_{2q} + \frac{R_{2q}}{L_{2q}} L''_{aqs} (-i_q + \frac{\psi_{1q}}{L_{1q}} + \frac{\psi_{2q}}{L_{2q}})] \quad \text{A.6}$$

Where,

$$L_d = \frac{X_d}{w_1} \quad \text{A.7}$$

$$L_q = \frac{X_q}{w_1} \quad \text{A.8}$$

$$L'_d = \frac{X'_d}{w_1} \quad \text{A.9}$$

$$L''_d = \frac{X''_d}{w_1} \quad \text{A.10}$$

$$L''_q = \frac{X''_q}{w_1} \quad \text{A.11}$$

$$L_l = \frac{X_l}{w_1} \quad \text{A.12}$$

$$L_{ad} = L_d - L_l \quad \text{A.13}$$

$$L_{aq} = L_q - L_l \quad \text{A.14}$$

$$L_{fd} = (L'_d - L_l) \times \frac{L_{ad}}{(L_{ad} - (L'_d - L_l))} \quad \text{A.15}$$

$$L_{1d} = (L_{sd} - L_l) \times \frac{L_{ad} \times L_{fd}}{(L_{ad} \times L_{fd} - (L_{sd} - L_l) \times (L_{ad} - L_{fd}))} \quad \text{A.16}$$

$$L_{1q} = (L'_q - L_l) \times \frac{L_{aq}}{(L_{aq} - (L'_q - L_l))} \quad \text{A.17}$$

$$L_{2q} = (L_{sq} - L_l) \times \frac{L_{aq} \times L_{1q}}{(L_{aq} \times L_{1q} - (L_{sq} - L_l) \times (L_{aq} - L_{1q}))} \quad \text{A.18}$$

$$R_{fd} = \frac{L_{ad} + L_{fd}}{T'_{d0} \times 314} \quad \text{A.19}$$

$$R_{1d} = \frac{1}{T''_{d0} \times 314} \times \frac{L_{1d} + (L_{fd} \times L_{ad})}{L_{fd} + L_{ad}} \quad \text{A.20}$$

$$R_{1q} = \frac{L_{aq} + L_{1q}}{T'_{q0} \times 314} \quad \text{A.21}$$

$$R_{2q} = \frac{1}{T''_{q0} \times 314} \times \frac{L_{2q} + (L_{aq} \times L_{1q})}{L_{aq} + L_{1q}} \quad \text{A.22}$$

$$L''_{ads} = \frac{1}{\frac{1}{L_{ad}} + \frac{1}{L_{fd}} + \frac{1}{L_{1d}}} \quad \text{A.23}$$

$$L''_{aqs} = \frac{1}{\frac{1}{L_{aq}} + \frac{1}{L_{1q}} + \frac{1}{L_{2q}}} \quad \text{A.24}$$

Generator parameters are as follows.

$R_a = 0.00228$	$X_d = 1.836$	$X_q = 1.790$	$X_{td} = 0.20$
$X_{tq} = 0.33$	$X_{sd} = 0.155$	$X_{sq} = 0.152$	$X_l = 0.124$
$T'_{d0} = 8$	$T''_{d0} = 0.03$	$T'_{q0} = 0.3371$	$T''_{q0} = 0.0295$

## A.2 Exciter Model

As discussed earlier, IEEE AC4 model is used for the exciter. The gain and the time constants used are as follows.

$$K_1 = 200 \quad T_a = 1 \quad T_b = 10 \quad T_e = 1 \quad V_{ref} = 1$$

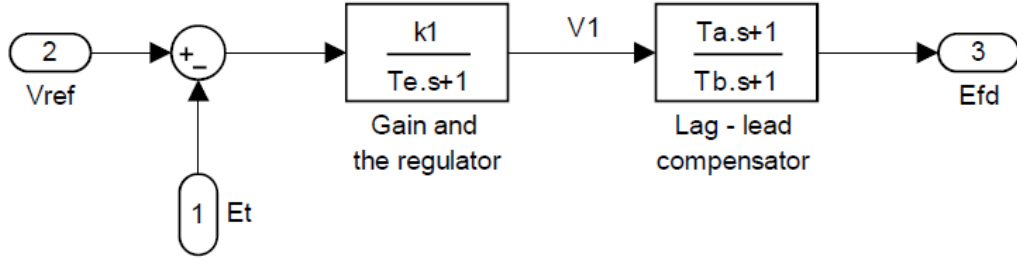


Figure A.1 : IEEE AC4 Exciter Model

$$\dot{V}_1 = \frac{1}{T_e} [-V_1 + k_1(V_{ref} - E_t)] \quad A.25$$

$$\dot{E}_{fd} = \frac{1}{T_b} [-E_{fd} + V_1 \left(1 - \frac{T_a}{T_e}\right) + \frac{k_1 T_a}{T_e} (V_{ref} - E_t)] \quad A.26$$

Where,

$$i_d = \frac{1}{\frac{1}{L_{f1d}} - \frac{1}{L_{ffd}}} \times \frac{1}{L_{ad}} \times \left( \frac{\psi_{fd} - L_{f1d} \times i_{1d}}{L_{ffd}} - \frac{\psi_{1d} - L_{11d} \times i_{1d}}{L_{f1d}} \right) \quad A.27$$

$$i_q = \frac{L_{11q} \times i_{1q} + L_{aq} \times i_{2q} - \psi_{1q}}{L_{aq}} \quad A.28$$

$$E''_d = -w_r \times L''_{aqs} \times \left( \frac{\psi_{1q}}{L_{1q}} + \frac{\psi_{2q}}{L_{2q}} \right) \quad A.29$$

$$E''_q = w_r \times L''_{ads} \times \left( \frac{\psi_{fd}}{L_{fd}} + \frac{\psi_{1d}}{L_{1d}} \right) \quad A.30$$

$$e_q = -R_a \times i_q - X_{sd} \times i_d + E''_q \quad A.31$$

$$e_d = -R_a \times i_d - X_{sq} \times i_q + E''_d \quad \text{A.32}$$

$$E_t = \left| \sqrt{e_d^2 + e_q^2} \right| \quad \text{A.33}$$

$E''_d$  and  $E''_q$  are the d – q axis components of the voltage applied to sub transient reactance.

### A.3 Network Model

As discussed in Chapter 2 network modelled using following positive sequence impedance values.

$$R = 0.02 \Omega/km \quad L = 0.8679 \times 10^{-3} \text{ H/km} \quad C = 13.41 \times 10^{-9} \text{ F/km}$$

$$Z_{base} = 137.11 \Omega$$

Base impedance value is calculated considering base voltage and the base apparent power value.  $Y_{bus}$  matrix is obtained for two scenarios i.e. for intact (Figure A.2) and one line outage (Figure A.2) condition.

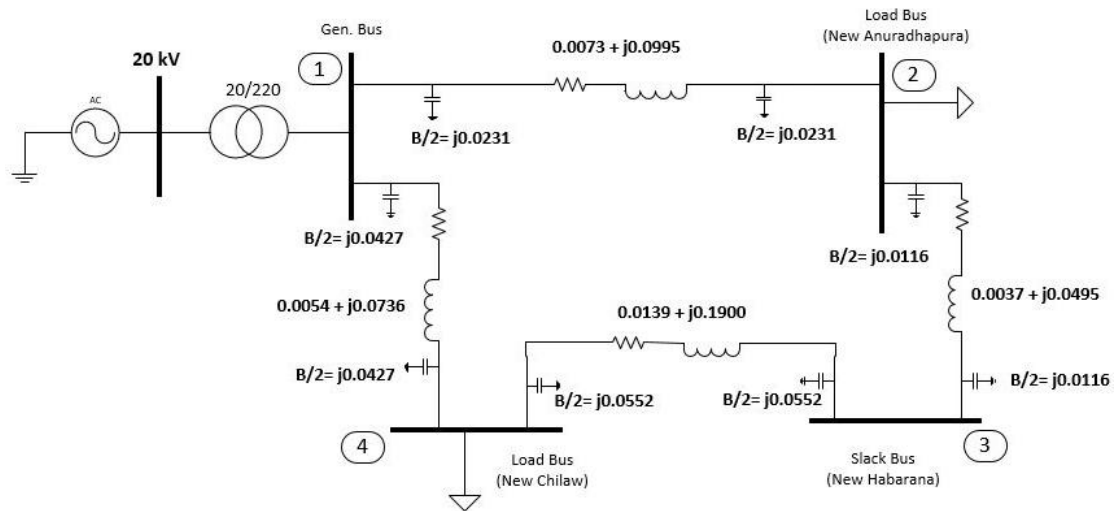


Figure A.2 : Network in Intact Condition

Consider  $Y_{\text{bus}}$  matrix,

$$Y_{\text{bus}} = \begin{bmatrix} Y_{11} & Y_{12} & Y_{13} & Y_{14} \\ Y_{21} & Y_{22} & Y_{23} & Y_{24} \\ Y_{31} & Y_{32} & Y_{33} & Y_{34} \\ Y_{41} & Y_{42} & Y_{43} & Y_{44} \end{bmatrix}$$

For the intact condition,

$$Y_{11} = 1.7236 - 23.5237i$$

$$Y_{13} = 0$$

$$Y_{21} = -0.733 + 9.9983i$$

$$Y_{23} = -1.4816 + 20.0928i$$

$$Y_{31} = 0$$

$$Y_{33} = 1.8653 + 25.2604i$$

$$Y_{41} = -0.9906 - 13.5112i$$

$$Y_{43} = -0.3837 + 5.2343i$$

$$Y_{12} = -0.733 + 9.9983i$$

$$Y_{14} = -0.9906 - 13.5112i$$

$$Y_{22} = 2.2146 - 30.0565i$$

$$Y_{24} = 0$$

$$Y_{32} = -1.4816 + 20.0928i$$

$$Y_{34} = -0.3837 + 5.2343i$$

$$Y_{42} = 0$$

$$Y_{44} = 1.3743 - 18.6476i$$

For the contingency condition,

$$Y_{11} = 0.9906 - 13.5485i$$

$$Y_{13} = 0$$

$$Y_{21} = 0$$

$$Y_{23} = -1.4816 + 20.0928i$$

$$Y_{31} = 0$$

$$Y_{33} = 1.8653 + 25.2604i$$

$$Y_{41} = -0.9906 - 13.5112i$$

$$Y_{43} = -0.3837 + 5.2343i$$

$$Y_{12} = 0$$

$$Y_{14} = -0.9906 - 13.5112i$$

$$Y_{22} = 1.4816 - 20.0813i$$

$$Y_{24} = 0$$

$$Y_{32} = -1.4816 + 20.0928i$$

$$Y_{34} = -0.3837 + 5.2343i$$

$$Y_{42} = 0$$

$$Y_{44} = 1.3743 - 18.6476i$$

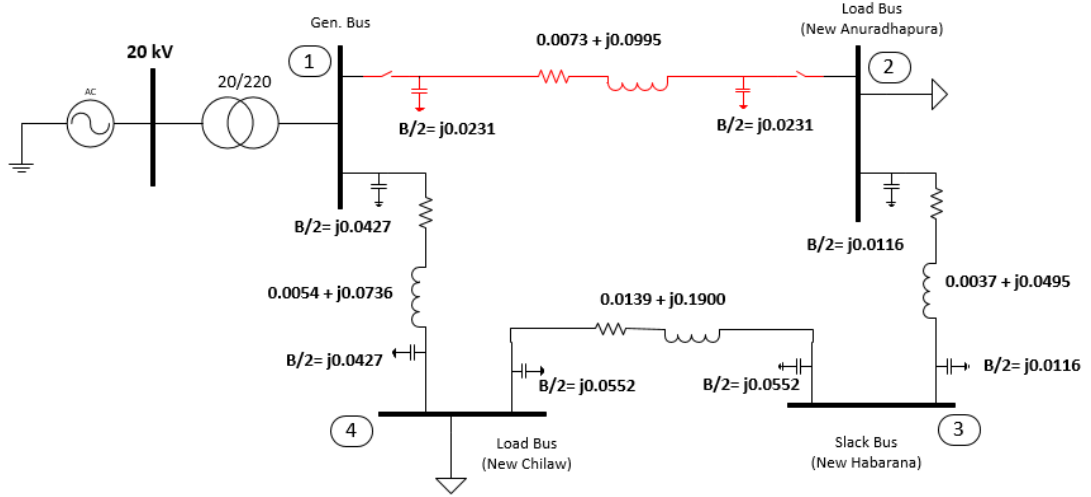


Figure A.3 : Network in Contingency Condition

#### A.4 Power Flow and Load Model

As discussed in Chapter 2, the dynamic load model used to model the loads. Calculated parameters were as follows.

For No 2 Load bus,

$$K_{pv} = 0.3 \quad K_{qv1} = 17.8 \quad K_{qv2} = 11.44 \quad K_{qw} = -0.03 \quad K_{pw} = 0.4$$

For No 4 Load bus,

$$K_{pv} = 0.3 \quad K_{qv1} = 4.8 \quad K_{qv2} = 4 \quad K_{qw} = -0.03 \quad K_{pw} = 0.4$$

Dynamic load model,

$$P = P_0 + P_1 + k_{pw} \delta + k_{pv} (V + TV) \quad \text{A.34}$$

$$Q = Q_0 + Q_1 + k_{qw} \delta + k_{qv1} V + k_{qv2} V^2 \quad \text{A.35}$$

Using the power flow equation real and reactive power supplied to the load can be calculated using,

$$P = - \sum_{i=1}^n |Y_{ki} V_i V_k| \cos(\theta_{ki} + \delta_i + \delta_k) \quad \text{A.36}$$

$$Q = \sum_{i=1}^n |Y_{ki} V_i V_k| \sin(\theta_{ki} + \delta_i + \delta_k) \quad \text{A.37}$$

In addition to Equations (A.1) to (A.6), (A.25) and (A.26), following power flow equations were derived (A.38 to A.45). These set of equations solved numerically using MATLAB to analyse the behaviour considering all the nonlinearities.

$$\dot{\delta}_2 = \frac{1}{k_{qw2}} \times \left( Q_{l2} - Q_{02} - P_{12} - (k_{qv12} \times \psi_{1d}) - (k_{qv22} \times V_2^2) \right) \quad \text{A.38}$$

$$\dot{V}_2 = \frac{1}{k_{qv2} \times T} \times \left( P_{l2} - P_{02} - P_{12} - (k_{pw2} \times \delta_2) - (k_{pv2} \times V_2) \right) \quad \text{A.39}$$

$$\dot{\delta}_4 = \frac{1}{k_{qw4}} \times \left( Q_{l4} - Q_{04} - P_{14} - (k_{qv14} \times V_2) - (k_{qv24} \times V_2^2) \right) \quad \text{A.40}$$

$$\dot{V}_4 = \frac{1}{k_{qv4} \times T} \times \left( P_{l4} - P_{04} - P_{14} - (k_{pw4} \times \delta_4) - (k_{pv4} \times V_2) \right) \quad \text{A.41}$$

$$P_2 = - \left( (E_m Y_{21} \cos(\theta_{21} + \delta - \delta_2) + E_0 Y_{23} \cos(\theta_{23} - \delta_2)) \times V_2 + Y_{22} \cos \theta_{22} V_2^2 \right) \quad \text{A.42}$$

$$Q_2 = \left( E_m Y_{21} \sin(\theta_{21} + \delta - \delta_2) + E_0 Y_{23} \sin(\theta_{23} - \delta_2) \right) \times V_2 + Y_{22} \sin(\theta_{22}) V_2^2 \quad \text{A.43}$$

$$P_4 = - \left( (E_m Y_{41} \cos(\theta_{41} + \delta - \delta_4) + E_0 Y_{43} \cos(\theta_{43} - \delta_4)) \times V_4 + Y_{44} \cos \theta_{44} V_4^2 \right) \quad \text{A.44}$$

$$Q_4 = \left( E_m Y_{41} \sin(\theta_{41} + \delta - \delta_4) + E_0 Y_{43} \sin(\theta_{43} - \delta_4) \right) \times V_4 + Y_{44} \sin \theta_{44} V_4^2 \quad \text{A.45}$$

## Appendix - B: Load Bus Data

Following 220 kV bus data from New Anuradhapura (NA) and New Chilaw (NC) substations were used to calculate corresponding gain values in dynamic load model.

### B.1 220 kV Load Bus – Weekend

Time	NA Receiving - Weekend				NC Receiving - Weekend			
	kV	A	MW	Mvar	kV	A	MW	Mvar
0:30	222	200	74	4	216	790	288	78
1:00	223	200	74	10	218	762	282	70
1:30	223	200	74	10	217	756	278	78
2:00	223	200	74	10	218	748	276	70
2:30	224	200	74	10	217	762	278	78
3:00	224	200	74	10	218	734	274	66
3:30	224	200	74	10	217	746	276	64
4:00	224	200	74	10	219	724	272	62
4:30	224	200	74	10	219	720	268	64
5:00	224	150	50	10	219	714	266	64
5:30	223	150	56	12	217	710	260	66
6:00	222	200	74	2	217	716	260	70
6:30	223	200	74	2	216	730	262	76
7:00	223	150	74	10	218	690	254	64
7:30	223	200	74	10	218	684	252	60
8:00	223	200	74	10	218	722	266	64
8:30	222	200	74	10	217	726	266	66
9:00	221	200	74	0	217	732	268	68
9:30	220	200	74	0	215	718	256	80
10:00	224	200	74	0	215	704	250	84
10:30	224	200	74	0	215	720	254	86
11:00	224	200	74	0	215	722	254	86
11:30	223	200	74	0	215	722	256	84
12:00	223	200	74	6	215	730	258	86
12:30	223	200	74	6	214	746	262	88
13:00	225	200	74	4	215	750	266	86
13:30	226	200	74	2	216	746	266	82
14:00	225	220	74	0	215	754	270	82
14:30	225	220	74	0	215	756	270	84
15:00	225	200	74	0	216	732	262	80
15:30	225	200	74	0	215	738	262	84
16:00	225	200	74	0	215	738	262	82
16:30	225	250	98	0	217	742	266	78

17:00	225	300	112	0	217	798	254	68
17:30	226	380	144	0	218	788	252	64
18:00	224	400	148	0	217	734	268	66
18:30	225	400	148	0	210	794	272	100
19:00	224	400	148	0	210	784	268	100
19:30	224	400	148	0	211	794	272	100
20:00	223	400	148	0	212	810	282	94
20:30	223	400	148	0	212	810	284	90
21:00	222	380	144	0	213	792	284	90
21:30	223	300	112	0	213	770	272	84
22:00	223	300	112	0	213	748	262	90
22:30	222	250	98	0	215	756	268	82
23:00	224	220	80	10	215	752	270	80
23:30	224	220	80	10	216	752	272	76
0:00	224	200	74	10	217	744	270	66

## B.2 220 kV Load Bus – Weekday

Time	NA Receiving - Weekday				NC Receiving - Weekday			
	kV	A	MW	Mvar	kV	A	MW	Mvar
0:30	224	280	100	20	215	971	324	99
1:00	224	400	140	20	216	938	296	99
1:30	224	400	140	20	217	820	292	146
2:00	224	400	140	20	216	819	293	105
2:30	224	400	140	20	215	861	300	118
3:00	224	400	140	20	216	833	300	106
3:30	224	400	140	20	215	852	308	102
4:00	224	400	140	20	217	999	313	122
4:30	224	400	140	20	216	931	329	115
5:00	224	420	148	20	215	1031	372	125
5:30	223	420	148	20	212	1076	385	149
6:00	222	460	152	20	217	1086	384	166
6:30	220	460	152	20	217	1083	385	152
7:00	220	440	152	20	222	1046	398	128
7:30	220	440	152	20	221	1094	395	153
8:00	219	400	150	0	221	1140	426	116
8:30	217	400	150	10	219	1090	407	138
9:00	221	400	150	10	222	1151	422	170
9:30	222	400	148	6	220	1138	401	185
10:00	223	400	148	0	220	1166	413	196
10:30	222	350	138	0	220	1213	427	184

11:00	222	350	138	0	219	1264	434	232
11:30	220	380	144	0	219	1267	443	201
12:00	220	400	148	0	214	1237	431	198
12:30	221	400	148	0	219	1214	438	187
13:00	221	400	148	0	219	1221	424	198
13:30	222	400	148	0	221	1202	426	195
14:00	221	400	148	0	219	1246	431	134
14:30	221	400	148	0	219	1240	436	211
15:00	221	350	138	0	220	1227	419	203
15:30	221	400	148	0	219	1208	418	215
16:00	220	400	148	0	220	1238	447	223
16:30	221	400	148	0	221	1196	420	201
17:00	222	400	148	0	221	1341	421	176
17:30	223	500	184	20	223	1298	419	181
18:00	221	550	204	8	219	1161	420	169
18:30	215	600	224	10	214	1154	395	192
19:00	216	600	224	10	215	1140	400	162
19:30	216	620	224	10	216	1154	401	162
20:00	217	600	224	8	217	1173	420	138
20:30	218	600	224	10	216	1206	422	162
21:00	219	580	220	10	217	1174	425	183
21:30	219	580	220	8	217	1124	405	143
22:00	220	550	204	10	217	1146	406	140
22:30	220	400	148	4	214	1206	428	139
23:00	221	380	144	4	214	1242	442	152
23:30	224	250	90	4	215	1228	438	155
0:00	225	220	80	10	219	806	296	84

## Appendix - C: MATLAB Code

MATLAB (R2015a) is used to model and analyse the behaviour of the system and several functions, with their source code, are listed below.

### C.1 $Y_{bus}$ Matrix

$Y_{bus}$  matrix is obtained using the following MATLAB code with the network data.

```
%Ybus matrix calculation for NA, NC, NH lines considering TF
impedance
%Zbase = 137.11

Y100 = 0.7330 - 9.9983i;      %Line sections with distance
Bc100 = 0.0231i;
Y74 = 0.9906 - 13.5112i;
Bc74 = 0.0427i;
Y50 = 1.4816 - 20.0928i;
Bc50 = 0.01155i;
Y191 = 0.3837 - 5.2343i;
Bc191 = 0.05516i;
Ytx = - 0.08i;

Y(1,1) = Y100 + Bc100 + Y74 + Bc74 + Ytx;
Y(1,2) = - Y100;
Y(1,3) = 0;
Y(1,4) = -Y74;

Y(2,1) = Y(1,2);
Y(2,2) = Y100 + Bc100 + Y50 + Bc50;
Y(2,3) = -Y50;
Y(2,4) = 0;

Y(3,1) = Y(1,3);
Y(3,2) = Y(2,3);
Y(3,3) = Y191 + Bc191 + Y50 + Bc50;
Y(3,4) = -Y191;

Y(4,1) = Y(1,4);
Y(4,2) = Y(2,4);
Y(4,3) = Y(3,4);
Y(4,4) = Y191 + Bc191 + Y74 + Bc74;

Ybus1 = vpa (Y , 10)          %Admittance in the complex form
rho=abs(Ybus1);
theta=angle(Ybus1);
vpa (rho , 10)
vpa (theta , 10)
angle1 = theta * (180/pi);
vpa (angle1 , 10)
```

## C.2 Power Flow Calculation

New function is defined to perform power flow calculation for the given data. Voltage variation in the bus under consideration is also analysed within the function.

```
function [ dx ] = Bus4var_Fun_2_Q4Vary_FinalWithExciter( x, Q4 )

Q0 = 0.026;
Q1 = 0.025;
Q40 = 0.085;

Kpv = 0.3;
Kqv1 = 17.80;
Kqv2 = 11.44;
Kqw = -0.03;
Kpw = 0.4;

Kpv4 = 0.3;
Kqv14 = 4.80;
Kqv24 = 4.0;
Kqw4 = -0.03;
Kpw4 = 0.4;

P0 = 0.6;
P1 = 0;
P40 = 0.6;
P4 = 0;
E0 = 2.5;
Em = 1;
Pm = 1;
Kd = 0.05;
M = 0.3;
T = 8.5;

% Network
Y11 = 23.58676024;
O11 = -1.49765624;

Y12 = 10.02513301;
O12 = 1.643977867;

Y21 = Y12;
O21 = O12;

Y13 = 0;
O13 = 0;

Y22 = 30.13792693;
O22 = -1.497247875;

Y23 = 20.14735095;
O23 = 1.644400973;
```

```

Y41 = 13.54746522;
O41 = 1.643982332;

Y14 = Y41;
O14 = O41;

Y43 = 5.248344709;
O43 = 1.643970375;

Y44 = 18.69821323;
O44 = -1.497230989;

% Main equations
P = - ((Em * Y21 * cos(O21 + x(1) - x(3)) + Y23 * E0 * cos(O23 -
x(3))) * x(4) + Y22 * cos(O22) * x(4)^2);
Q = (Em * Y21 * sin(O21 + x(1) - x(3)) + Y23 * E0 * sin(O23 -
x(3))) * x(4) + (Y22 * sin(O22) * x(4)^2);

PP = - ((Em * Y41 * cos(O41 + x(1) - x(5)) + Y43 * E0 * cos(O43 -
x(5))) * x(6) + (Y44 * cos(O44) * x(6)^2));
QQ = (Em * Y41 * sin(O41 + x(1) - x(5)) + Y43 * E0 * sin(O43 -
x(5))) * x(6) + (Y44 * sin(O44) * x(6)^2);

Pe = (Em^2 * Y11 * cos(O11) + Y12 * Em * x(4) * cos(O12 + x(3) -
x(1)) + Y14 * Em * x(6) * cos(O14 + x(5) - x(1)));
Qe = -((Em^2 * Y11 * sin(O11) + Y12 * Em * x(4) * sin(O12 + x(3) -
x(1)) + Y14 * Em * x(6) * sin(O14 + x(5) - x(1))));

dx(1) = x(2);
dx(2) = (1/M) * (-Kd*x(2) + Pm - Pe) ;

dx(3) = (1/Kqw) * (Q - Q0 - Q1 - (Kqv1 * x(4)) - (Kqv2 * x(4)^2));
dx(4) = (1/(Kpv * T)) * (P - P0 - P1 - (Kpw * dx(3)) - (Kpv *
x(4)));

dx(5) = (1/Kqw4) * (QQ - Q40 - Q4 - (Kqv14 * x(6)) - (Kqv24 *
x(6)^2));
dx(6) = (1/(Kpv4 * T)) * (PP - P40 - P4 - (Kpw4 * dx(5)) - (Kpv4 *
x(6)));

w0 = 314;
f = 50;
w = 2 * pi * f;

% Gen parameters
Ra = 0.00228;
Xd = 1.836;
Xq = 1.79;
Xtd = 0.2;
Xtq = 0.33;
Xsd = 0.155;
Xsq = 0.152;
Xl = 0.124;
Ttd0 = 8;
Tsd0 = 0.03;

```

```

Ttq0 = 0.3371;
Tsq0 = 0.0295;

Ld = Xd/w;
Lq = Xq/w;
Ltd = Xtd/w;
Ltq = Xtq/w;
Lsd = Xsd/w;
Lsq = Xsq/w;
Ll = Xl/w;

Lad = Ld - Ll;
Laq = Lq - Ll;

Lfd = (Ltd - Ll) * (Lad) / (Lad - (Ltd - Ll));
Lld = (Lsd - Ll) * (Lad * Lfd) / (Lad * Lfd - (Lsd - Ll) * (Lad + Lfd));
Llq = (Ltq - Ll) * (Laq) / (Laq - (Ltq - Ll));
L2q = (Lsq - Ll) * (Laq * Llq) / (Laq * Llq - (Lsq - Ll) * (Laq + Llq));

Rfd = (Lad + Lfd) / (Ttd0 * 314);
Rld = (1/(Tsd0 * 314)) * (Lld + (Lfd * Lad) / (Lfd + Lad));
R1q = (Laq + Llq) / (Ttq0 * 314);
R2q = (1/(Tsq0 * 314)) * (L2q + (Laq * Llq) / (Laq + Llq));

L2ads = 1 / ((1/Lad) + (1/Lfd) + (1/Lld));
L2aqs = 1 / ((1/Laq) + (1/Llq) + (1/L2q));

L2ad = L2ads;
L2aq = L2aqs;

% Exciter parameters
wr = 1;
L11q = L1q + Laq;
Lffd = Lfd + Lad;
Lf1d = Lffd - Lfd;
L11d = L1d + Lf1d;

Ta = 1;
Tb = 10;
Te = 1;
Kl = 200;

id = (1/((1/Lf1d) - (1/Lffd))) * (1/Lad) * ((x(7) - Lf1d * i1d) / Lffd - ((x(8) - L11d * i1d) / Lf1d));
iq = (L11q * i1q + Laq * i2q - x(9)) / Laq;

% Generator other equations
dx(7) = ((w0 * Rfd)/Lad) * x(12) - ((w0 * Rfd)/Lfd) * x(7) + ((w0 * Rfd)/Lfd) * (L2ads * (-id + (x(7)/Lfd) + (x(8)/L1d)));
dx(8) = -w0 * ((Rld/L1d) * x(7) + (Rld/L1d) * (L2ads * (-id + (x(7)/Lfd) + (x(8)/L1d))));

```

```

dx(9) = w0 * ( (-R1q/L1q) * x(9) + (R1q/L1q) * (L2aqs * (-iq
+(x(9)/L1q) + (x(10)/L2q))));
dx(10) = w0 * ( (-R2q/L2q) * x(10) + (R2q/L2q) * (L2aqs * (-iq
+(x(9)/L1q) + (x(10)/L2q))));

% Currents
i1d = - dx(8)/R1d;
i1q = - dx(9)/R1q;
i2q = - dx(10)/R2q;

E2d = - wr * L2aq * ((x(9)/L1q) + (x(10)/L2q));
E2q = wr * L2ad * ((x(7)/Lfd) + (x(8)/L1d));

eq = -Ra * iq - Xsd * id + E2q;
ed = -Ra * id - Xsq * iq + E2d;

Et = (abs( sqrt ( eq^2 + ed^2 )))/20;
Vref = 1;

% Exciter equations
dx(11) = (1/Te) * (-x(11) + K1 * (Vref - Et));
dx(12) = (1/Tb) * (Ta * dx(11) + x(11) - x(12));

end

```

### C.3 Eigenvalue Movements

Following code is used to analyse the eigenvalue behaviour with respect to the different loading conditions.

```

%Eigenvalue Movement
syms Q4 v u w z r t g h b c e f      %Symbolic parameters
%System data
Q0 = 0.026;
Q1 = 0.025;
Q40 = 0.085;

Kpv = 0.3;
Kqv1 = 17.80;
Kqv2 = 11.44;
Kqw = -0.03;
Kpw = 0.4;

Kpv4 = 0.3;
Kqv14 = 4.80;
Kqv24 = 4.0;
Kqw4 = -0.03;
Kpw4 = 0.4;

P0 = 0.6;
P1 = 0;
P40 = 0.6;

```

```

P4 = 0;
E0 = 2.5;
Em = 1;
Pm = 1;
Kd = 0.05;
M = 0.3;
T = 8.5;

Y11 = 23.58676024;
O11 = -1.49765624;

Y12 = 10.02513301;
O12 = 1.643977867;

Y21 = Y12;
O21 = O12;

Y13 = 0;
O13 = 0;

Y22 = 30.13792693;
O22 = -1.497247875;

Y23 = 20.14735095;
O23 = 1.644400973;

Y41 = 13.54746522;
O41 = 1.643982332;

Y14 = Y41;
O14 = O41;

Y43 = 5.248344709;
O43 = 1.643970375;

Y44 = 18.69821323;
O44 = -1.497230989;

% Main equations
P = - ((Em * Y21 * cos(O21 + u - w) + Y23 * E0 * cos(O23 - w)) * z +
(Y22 * cos(O22) * z^2));
Q = (Em * Y21 * sin(O21 + u - w) + Y23 * E0 * sin(O23 - w)) * z +
(Y22 * sin(O22) * z^2);

PP = - ((Em * Y41 * cos(O41 + u - r) + Y43 * E0 * cos(O43 - r)) * t
+ (Y44 * cos(O44) * t^2));
QQ = (Em * Y41 * sin(O41 + u - r) + Y43 * E0 * sin(O43 - r)) * t
+ (Y44 * sin(O44) * t^2);

Pe = (Em^2 * Y11 * cos(O11) + Y12 * Em * z * cos(O12 + w - u) +
Y14 * Em * t * cos(O14 + r - u));
Qe = -((Em^2 * Y11 * sin(O11) + Y12 * Em * z * sin(O12 + w - u) +
Y14 * Em * t * sin(O14 + r - u)));

du = v;

```

```

dv = (1/M) * (-Kd*v + Pm - Pe) ;

dw = (1/Kqw) * (Q - Q0 - Q1 - (Kqv1 * z) - (Kqv2 * z^2));
dz = (1/(Kpv * T)) * (P - P0 - P1 - (Kpw * dw) - (Kpv * z));

dr = (1/Kqw4) * (Q0 - Q40 - Q4 - (Kqv14 * t) - (Kqv24 * t^2));
dt = (1/(Kpv4 * T)) * (PP - P40 - P4 - (Kpw4 * dr) - (Kpv4 * t));

w0 = 314;
freq = 50;
w1 = 2 * pi * freq;

% Gen parameters
Ra = 0.00228;
Xd = 1.836;
Xq = 1.79;
Xtd = 0.2;
Xtq = 0.33;
Xsd = 0.155;
Xsq = 0.152;
Xl = 0.124;

Ttd0 = 8;
Tsd0 = 0.03;
Ttq0 = 0.3371;
Tsq0 = 0.0295;

Ld = Xd/w1;
Lq = Xq/w1;
Ltd = Xtd/w1;
Ltq = Xtq/w1;
Lsd = Xsd/w1;
Lsq = Xsq/w1;
Ll = Xl/w1;

Lad = Ld - Ll;
Laq = Lq - Ll;

Lfd = (Ltd - Ll) * (Lad) / (Lad - (Ltd - Ll));
Lld = (Lsd - Ll) * (Lad * Lfd) / (Lad * Lfd - (Lsd - Ll) * (Lad + Lfd));
Llq = (Ltq - Ll) * (Laq) / (Laq - (Ltq - Ll));
L2q = (Lsq - Ll) * (Laq * Llq) / (Laq * Llq - (Lsq - Ll) * (Laq + Llq));

Rfd = (Lad + Lfd) / (Ttd0 * 314);
R1d = (1/(Tsd0 * 314)) * (Lld + (Lfd * Lad) / (Lfd + Lad));
R1q = (Laq + Llq) / (Ttq0 * 314);
R2q = (1/(Tsq0 * 314)) * (L2q + (Laq * Llq) / (Laq + Llq));

L2ads = 1 / ((1/Lad) + (1/Lfd) + (1/Lld));
L2aqs = 1 / ((1/Laq) + (1/Llq) + (1/L2q));

L2ad = L2ads;
L2aq = L2aqs;

```

```

% Exciter parameters
wr = 314;
L11q = L1q + Laq;
Lffd = Lfd + Lad;
Lf1d = Lffd - Lfd;
L11d = L1d + Lf1d;

Ta = 1;
Tb = 10;
Te = 0.5;
K1 = 200;

i1d = 0;
i1q = 0;
i2q = 0;

id = (1/((1/Lf1d) - (1/Lffd))) * (1/Lad) * ( (g - Lf1d * i1d) /
Lffd) - ((h - L11d * i1d) / Lf1d));
iq = (L11q * i1q + Laq * i2q - b) / Laq;

% Generator other equations
dg = ((w0 * Rfd)/Lad) * f) - ((w0 * Rfd)/Lfd) * g + ((w0 *
Rfd)/Lfd) * (L2ads * (-id + (g/Lfd) + (h/L1d)));
dh = -w0 * ( (R1d/L1d)*g + (R1d/L1d) * (L2ads * (-id + (g/Lfd) +
(h/L1d))));

db = w0 * ( (-R1q/L1q)*b + (R1q/L1q) * (L2aqs * (-iq + (b/L1q) +
(c/L2q))));
dc = w0 * ( (-R2q/L2q)*c + (R2q/L2q) * (L2aqs * (-iq + (b/L1q) +
(c/L2q))));

E2d = - wr * L2aq * ((b/L1q) + (c/L2q));
E2q = wr * L2ad * ((g/Lfd) + (h/L1d));

eq = -Ra * iq - Xsd * id + E2q;
ed = -Ra * id - Xsq * iq + E2d;

Et = (abs( sqrt ( eq^2 + ed^2 )));
Vref = 1;

% Exciter equations
de = (1/Te) * (-e + K1 * (Vref - Et));
df = (1/Tb) * (Ta * de + e - f);

fun = @Bus4var_Fun_2_Q4Vary_FinalWithExciter;
clear m;
i = 0;

for Q4 = 1 %any given Q4 value
    i = i +1;
    x0 = [0, 0, 0, 1, 0, 1, 1, 1, 0, 0, 1, 1];
    options = optimset('MaxIter',10000,'MaxFunEvals',10000);
    x = fsolve(@(x)fun(x,Q4), x0, options);
    vpa (x , 5);

```

```

    m(i,:) = [ x(1), x(2), x(3), x(4), x(5), x(6), x(7), x(8), x(9),
x(10), x(11), x(12), Q4];
end

[rows, columns] = size (m);
eqns = [du dv dw dz dr dt dg dh db dc de df];
jac = jacobian ([eqns], [u , v , w , z , r , t, g, h, b, c, e, f]);
clear jacob;

for j = 1 : rows
jacS = subs (jac, {u , v , w , z , r , t, g, h, b, c, e, f},
{m(j,1), m(j,2), m(j,3), m(j,4), m(j,5), m(j,6), m(j,7), m(j,8),
m(j,9), m(j,10), m(j,11), m(j,12)});
eg = eig (jacS);
k = vpa (eg , 4);
jacob(j,:) = [ k(1,1), k(2,1), k(3,1), k(4,1), k(5,1), k(6,1),
k(7,1), k(8,1), k(9,1), k(10,1), k(11,1), k(12,1) m(j,13)];
end
vpa (jacob , 4)

```